A. L. LONDON

NATIONAL ADVISORY COMMITTEE FOR AERONAUTICS

TECHNICAL NOTE

No. 1003

THE THEORETICAL FLOW OF A FRICTIONLESS, ADIABATIC, PERFECT GAS INSIDE OF A TWO-DIMENSIONAL HYPERBOLIC NOZZLE

By Howard W. Emmons
Harvard University

NASA LIBRARY
AMES RESEARCH CENTER
MOFFETT FIELD, CALIF.

Washington
May 1946

COPY NO. 2

NATIONAL ADVISORY COMMITTEE FOR AERONAUTICS

TECHNICAL NOTE NO. 1003

THE THEORETICAL FLOW OF A FRICTIONLESS, ADIABATIC, PERFECT GAS INSIDE OF A TWO-DIMENSIONAL HYPERBOLIC NOZZLE

By Howard W. Emmons

SUMMARY

The two-dimensional flow of a frictionless, adiabatic, perfect gas inside of a two-dimensional hyperbolic nozzle has been studied by numerical methods described in NACA Technical Note No. 932. A series of solutions are presented which show an almost continuous transformation of known subsonic solutions to the known subsonic-supersonic solution. The words "almost continuous" are used because difficulties at the point where the shock waves touch the wall seem to prohibit continuous transformation from one type of solution to the next.

Solutions with partial shocks, that is, shock waves that do not extend all the way across the nozzle, are very hard to obtain. Residuals of one part in one thousand can sometimes be eliminated only by introducing a shock. The type of solution obtained is, thus, very sensitive to small changes in nozzle form.

The solutions are not single-valued, in general, in the relation of flow through the nozzle to pressure at a given point in the nozzle. In experiments, the flow might make small jumps as the type of flow pattern passes through unstable regions.

A few schlieren photographs show that the actual flow through this nozzle differs considerably from the computed solutions. All the differences can be ascribed to the effects of friction. Since the flow pattern in the nozzle is very critical in the slightly supersonic regions, the phenomena would be greatly altered if a boundary layer were included in the computation.

It has been known for some years that the perfect fluid theory, $p = f(\rho)$, was not adequate to describe any of the phenomena during transition from wholly subsonic to subsonic-supersonic flow in a nozzle. For a one-dimensional theory, shock waves together with an otherwise perfect fluid are enough. From this report it can be concluded that for the corresponding two-dimensional problem a perfect fluid theory supplemented with shock waves is still not enough. For adequate check with experiment, a theory must be based upon a fluid with friction (at least in regions near the walls; in other regions friction would have no effect). Solutions with this imperfect fluid involve a prohibitive amount of labor with present computing techniques.

INTRODUCTION

The flow of compressible fluids through nozzles has been the subject of investigation, both experimental and theoretical, for more than a century. Nearly all the theoretical work has been confined to considerations of the flow of perfect gases, generally neglecting friction and heat transfer, although some work covering these latter effects has been attempted. Many of the early results are summed up in reference 1. Like all complicated physical problems, the first theoretical attacks are made with an oversimplified physical picture. In the case of flow through nozzles this simplification of fluid properties is used together with a simplified geometry. This assumes a one-dimensional treatment of the flow in the sense that velocity and fluid properties are assumed to be unique functions of a single variable which represents distance along the nozzle axis, the variation in nozzle cross section being taken normal to this axis or in some other but equally arbitrary manner. The one-dimensional theory shows that a simple converging-diverging nozzle acts for low velocities like a conventional venturi meter; that is, the velocity increases and the pressure decreases to the minimum section, following which the reverse occurs. As the exit pressure of the nozzle is lowered, the velocity at the minimum section continues to increase until a velocity equal to the local speed of sound appears.

In figure 1 the pressure variation along an arbitrary nozzle is plotted, showing the region for which the flow is similar to a conventional venturi meter. With further drop

in nozzle exit pressure the velocity at the diverging portion of the nozzle immediately following the throat increases above that of the speed of sound and continues thus to increase until interrupted by a shock wave. The standing shock wave adjusts its position in such a way that the fluid after the shock wave can continue through the nozzle to come out at the specified exit pressure. If the exit of the nozzle is considered infinitely far away, the shock wave can be moved as far from the minimum section as desired. If the nozzle is short, the shock wave eventually arrives at its end, then passes out of the nozzle in a complex manner. The phenomena occurring outside of the nozzle will not be considered in this report. Consider what happens inside of the nozzle when a better geometric approximation to its form is assumed.

The simplest improvement in assumption about the geometry of a nozzle is to consider a two-dimensional passage, that is, a passage like that drawn in figure 1, except that it will not be assumed that velocity and fluid properties are constant across some arbitrarily drawn cross section. In a recent work (reference 2) a refinement of the one-dimensional treatment which is good in the neighborhood of the nozzle axis was studied. No attempt was made to investigate solutions when shock waves were present, and no discussion is given of the transition from subsonic to subsonic-supersonic type of flow. Some work in this direction has been attempted. (See references 3, 4, and 5.) In each case the differential equations describing the two-dimensional motion of a frictionless, adiabatic, irrotational perfect gas are written for the region where the Mach number equals 1 and solutions are sought in the form of power series. Very considerable labor is required to evaluate the coefficients of the power series and, consequently, the power series were terminated at approximately the eighth power term. G. I. Taylor (reference 3) has studied in this way the symmetrical flow through a symmetrical passage. Thus, his solutions either are completely subsonic, that is, like the conventional venturi meter, or contain symmetrical supersonic regions located in the minimum section at the wall. As a result of this work it was shown that this type of solution was limited in a way which depended upon the curvature of the wall. T. Meyer (reference 4) has studied the nonsymmetrical flow through a nozzle which passed through the speed of sound from subsonic to supersonic. The solutions of Taylor and Meyer are sketched in figure 2a and 2e, respectively. Neither of these workers gave any indication of how the flow could change from the one form to the other. The generalization of the results of the one-dimensional theory is not

immediate since a shock wave at subsonic velocity is impossible and the solutions of Taylor do not include supersonic regions that extend completely across the passage. It is, therefore, impossible to assume with the one-dimensional theory that a minute shock appears at $M = 1$ (at minimum section) and then grows as the exit pressure is dropped. An attempt to fill the gap by the same power series method has been made by H. Görtler (reference 5), who used power series which permitted nonsymmetrical solutions and showed that solutions could be obtained which satisfied the differential equation up to the eighth degree terms used. Görtler does not show, however, that solutions of this form have any direct bearing upon what actually happens since he does not show that his series, even if continued to infinity, could actually represent solutions to the differential equation. It is now to be expected on the basis of results of other investigations, such as those of Ringleb (reference 6), that beyond the limit solution of Taylor there only exist solutions with cusps and overlapping streamlines which, of course, are of no physical significance. The results of Görtler's work, however, are suggestive in that the form of the constant velocity lines obtained by him indicates that the eighth degree equations are attempting to give a compression shock, but, of course, are unable to do so. It is easily conjectured, therefore, that the transition from the symmetrical type of flow of Taylor to the nonsymmetrical flow of Meyer takes place somewhat as indicated in figures 2b, 2c, and 2d. A small compression shock would be imagined as starting at the wall in Taylor's solution at the down stream point where the constant velocity $M = 1$ line arrives at the wall. It then grows in magnitude and extends toward the center of the passage. Eventually the shocks from opposite walls arrive at the center of the passage, combine and move as a single shock on downstream similar to the one-dimensional theory. This picture, as it turns out, is approximately correct, although certain modifications have still to be considered in future work.

This investigation, conducted at Harvard University, was sponsored by and conducted with the financial assistance of the National Advisory Committee for Aeronautics.

The author wishes to acknowledge indebtedness to Dr. Andrew Vazsonyi who carried out all the detailed computations and supplied many ideas during the hours of discussion of various fine points of the computations and the fluid mechanics.

SYMBOLS

a	accustic velocity
D	half nozzle throat dimension
M	Mach number
p	pressure
Pr	Prandtl number
q	velocity (components u, v)
Q	residual
R,r	radius of curvature of streamline
w	complex-velocity potential
x,y	coordinates in physical plane
z	complex coordinate in physical plane
α	angle between ψ and η lines
γ	isentropic exponent
δ	lattice spacing in computation
ϵ	fraction of lattice spacing from net point to shock wave
φ	deflection angle of streamline produced by an oblique shock
ψ	stream function
η	stream function for incompressible fluid
ξ	velocity potential for incompressible fluid
θ_w	oblique shock angle
ρ	mass density

ω	rate of rotation
$\omega' = \frac{\omega D}{a_o}$	dimensionless rotation

Subscripts

a	condition after a shock wave
b	condition before a shock wave
cr	critical condition
i	incompressible
ξ,η	denote differentiation in the corresponding direction
o,1,2,3,4,5	lattice points
o	stagnation condition

RESULTS OF RELAXATION SOLUTION OF THE FLOW THROUGH A HYPERBOLIC NOZZLE

Reference 7 shows how to apply the relaxation method to the solution of compressible fluid flow problems in two dimensions. A simple channel was chosen for first investigation, so that attention could be concentrated on the difficulties of the compressible fluids part of the problem without being bothered by difficult geometry. As a consequence, the channel formed by two hyperbolas was chosen. The complex potential function for this nozzle is

$$w = \sinh^{-1} z \tag{1}$$

where

$z = x + i\,y$

$w = \xi + i\,\eta$

ξ velocity potential

η stream function

The physical shape of this nozzle in the x,y plane is easily computed from

$$\left.\begin{aligned} x &= \sinh \xi \cos \eta \\ y &= \cosh \xi \sin \eta \end{aligned}\right\} \tag{2}$$

while the velocity q_i of an incompressible fluid flowing through this passage is given by

$$\frac{1}{q_i^2} = \frac{\cosh 2\xi + \cos 2\eta}{2} \tag{3}$$

Figure 3 shows the ξ and η lines in this nozzle. These lines are the coordinate system used in the compressible flow solutions. Figure 4 shows the flow of an incompressible fluid through this passage. This solution is to be compared with later solutions for the flow of compressible fluid at high velocity. All the remaining figures (5 through 30) show various facts about the flow of a gas through this nozzle while table I summarizes various numerical details. It should be observed that the flow is essentially that of a conventional venturi meter for all cases in which the Mach number at the center of the minimum section is $M \leq 0.812$. This is the limiting case essentially as would have been described by the solutions of Taylor. By graphical interpolation (fig. 9) it was found that $M = 1$ first appears at the wall for a center Mach number of 0.772. The appearance of $M = 1$ at the nozzle wall is in no way critical for the flow through the nozzle. It is of interest only because it formerly was, and occasionally still is, erroneously associated with some critical aspect of the flow. Shock waves do not, and indeed could not, occur when only one point has reached the local sonic velocity.

The essentially subsonic flows of figures 4 through 8 are equivalent to the results recently published by Southwell, Greene, and Fox (references 8 and 9) except for a different nozzle shape. The work of these two papers and the present report were carried out entirely independently and the extent to which the results agree is gratifying.

Before the solutions with shocks are discussed, it should be observed that the computer has a choice of the type of shock wave he wishes to consider. Should shock

TABLE I

THE MACH NUMBER AT VARIOUS POINTS IN THE NOZZLE

Figure	M Center of nozzle throat ($\xi = \eta = 0$)	M Center line at $\frac{x}{D} = 0.93$ ($\xi = 0.6$, $\eta = 0.0$)	M Wall at $x = 0$ ($\xi = 0.0$, $\eta = 0.6$)	M Maximum in nozzle	Remarks
4	0	0	0		Subsonic
5	.600	.46	.742		Subsonic
6	.692	.505	.875		Subsonic
	.772		1.000		By interpolation
7	.793	.540	1.035		Symmetrical
8	.812	.555	1.085		Subsonic-supersonic
10	.832	.556	1.133	1.143	Partial shocks
11	.875	.563	1.140	1.187	Partial shocks
12	0.932	.575	1.154	1.398	Partial shocks / Complete shocks
13	0.932	.602	1.154	1.443	Complete shocks
14	0.932	.625	1.154	1.525	Complete shocks
15	0.932	.642	1.154	1.63	Complete shocks
16	0.932	1.455	1.154	∞	Complete subsonic-supersonic solution

waves be normal or oblique? At the wall the immediate thought is to use only normal shocks since, then, the direction of the stream is unaltered on crossing the shock and hence the stream continues along the wall. As will be discussed later, a streamline curvature jump occurs across the shock which requires a curvature singularity in the subsonic flow following the shock. This singularity arises naturally during the course of the relaxation solution. If an oblique shock had been used, solutions could have been obtained which would have included a singularity, in some cases a stagnation point, downstream from the shock wave. In this report it was decided to use only normal shocks at the wall. In an actual nozzle, the boundary layer would alter the shock boundary condition considerably.

Figures 10 through 12 show solutions with partial shocks, that is, shocks that do not extend all the way across the nozzle. Figure 12 is included in this category in spite of the fact that the shock is drawn to extend completely across the nozzle. This case is a solution for which the shock waves from oppsite walls have just combined. The shock waves are here tangent to the $M = 1$ line at the center line of the channel. Thus, the shock waves become infinitesimal in magnitude. In the numerical work from which this solution was drawn, much higher accuracy would have been needed to distinguish between the solution as drawn and the solutions obtained, by merely erasing a small section of the shock and $M = 1$ line at the center of the nozzle. In other words, with a stream function of the order of 20,000 at the wall compared to zero at the center line there is not sufficient accuracy to distinguish precisely when the shock waves first combine. In figures 12 through 16 the shock wave is gradually moving down the nozzle essentially as predicted by the one-dimensional theory.

The first fact to be observed about these solutions with shock waves is the fact that they are not normal but curve upstream toward the center of the passage. In the course of obtaining solutions normal shock waves were inserted in the passage in what was considered the proper location. During the course of solution these shock waves had to be moved and made oblique by the processes described in appendix I in order to eliminate the residuals. As a first approximation it might be observed that the shock waves must curve so that the rate of change of entropy normal to the streamlines gives rise to a sufficient magnitude of rotation term of the differential equation to replace the density

terms of the differential equation which decrease discontinuously across the shock wave. The photograph (fig. 17) taken in a high-speed wind tunnel at Harvard University illustrates such a shock.

In figure 17 there is also shown another photograph at the "same" condition on a different day taken in 4 microseconds with a schlieren system. The phenomenon of many shocks is a nonsteady one probably associated with the turbulence of the air stream. Small "turbulence" pressure waves unable to pass through the throat accumulate there until they become a shock wave of sufficient magnitude to pass through. It should not be inferred that the partial shocks of the solutions are of no importance because they were not found in these nozzle experiments. For an airfoil in free flight only partial shocks are possible. After complete shocks are formed, agreement between wind-tunnel and free-flight conditions could not be expected.

Everything in these solutions appears to follow essentially the conjectured progress of development and growth of the shock waves. (See fig. 2.) That this is not quite correct can be seen by examining figures 8 and 10 more closely. It will be observed that the shock wave seems to arise (fig. 10) not at the point where the $M = 1$ line touches the wall (fig. 8) but somewhat upstream of this point, and, in fact, makes a sudden appearance (not starting with zero length near the wall). This can also be seen from the dotted line in figures 20 and 21. The changes that take place as the flow conditions are changed are shown again in figures 18 through 21, where the variation of Mach number and pressure along the center line and along the wall are shown. The variation in Mach number near the wall is shown in figure 10. It will be observed that the Mach number and pressure distributions along the wall proceed smoothly up to a shock wave. They then, of course, must change abruptly to the subsonic value appropriate to a shock wave at the correct angle (in this case normal) for the Mach number existing ahead of the shock. The pressure and Mach number do not vary smoothly from this value, however, but are shown with a discontinuous change on the subsonic side of the shock. For the solutions presented in this report, the Mach numbers at all net points along the wall on the subsonic side of the shock wave fell on a smooth curve which when extrapolated gave the discontinuities shown. For the row of net points adjacent to the wall no peculiar phenomena were required to get a solution. Later work, not reported here, has produced cases in which

the Mach number rises very steeply from the value after the shock and then turns smoothly into the descending Mach number curve. Thus it appears that the curves of this report should show a steep rise rather than the discontinuities.

Although the precise nature of the singularity at the wall in the subsonic flow following a shock has not been determined, there is no difficulty in finding the qualitative explanation of this phenomenon. Consider the supersonic flow of a compressible fluid along the convex side of a wall of given radius of curvature. In order that the fluid follow the wall there must be adjacent to the wall a normal component of pressure gradient such that the pressure increases away from the wall. This pressure gradient is required to turn the velocity vector as the fluid moves along the curved wall. If, now, a shock wave stands across this flow and reaches the curved wall, the stream ahead of the shock is left unaltered. The stream immediately behind the wave is determined by the shock wave conditions. The pertinent condition for the present considerations is the fact that, except for modifications caused by the entropy change, the lower the pressure (the higher the velocity) before a normal shock the higher the pressure immediately following the shock. Since the pressure before the shock increases away from the wall, the pressure after the shock will decrease away from the wall. Hence the streamlines <u>immediately</u> behind the shock must be curved away from the wall.

For the solutions presented in this report, the fluid was required to follow the wall. The streamlines behind the shock must, therefore, reverse their curvature in such a way that the inflection point approaches the shock wave as one moves closer to the nozzle wall; while at the wall, the inflection point coincides with the shock wave. In a qualitative sense, therefore, the subsonic flow behind the shock wave is similar to the isentropic flow of a fluid along a wall with a discontinuity of radius of curvature. The flow of an incompressible perfect fluid along a wall with a discontinuity of radius of curvature has been studied (reference 10) and leads to an infinite rate of change of velocity along the wall. Thus there is a singularity in the flow of an incompressible fluid along a wall with a jump in curvature of the same type as that found in the subsonic flow following a shock wave.

In the explanation of the wall singularity in the subsonic flow following a shock wave, it was noted that the

entropy jump through a shock would cause some modification of the explanation. On figure 22 the ratio of the radius of curvature of a streamline before and after a normal shock is shown as a function of the Mach number before the shock, taking into account the changes of entropy as they actually occur. Only at one Mach number is it possible for the stream to continue along a wall (with continuous curvature) without a singularity, and that is at a Mach number given by equation (22), which for air with $\gamma = 1.40$ is at $M = 1.66$.

An infinite rate of rise of pressure along any streamline adjacent to the wall is not possible because of the second law of thermodynamics which prevents an expansion shock. By writing the equation of continuity, momentum, and energy for a stream tube element enclosing a standing wave, there is found to be one and only one permissible subsonic state for each initial state, provided it is permissible to use an element the length of which in the direction of the streamlines is of higher order than its width. To find out what can happen <u>at</u> the wall, it is necessary to use a stream tube element with the wall as one side and with a width of the same (or higher) order as the length. If such an element is used, the effects on its sides are of the same order as the effects on its ends, and, consequently, the conclusions about unique state after the wave do not follow.

The rapid rise in Mach number along the wall after a shock wave varies in severity with both the wall curvature and the initial Mach number. In figure 23 the ratio of the Mach numbers before and after this rapid rise is plotted against the Mach number before the shock. There is also plotted the ratio of Mach numbers across a normal shock. It appears that for the present nozzle the rapid rise of Mach number following a shock caused by the curvature singularity would just compensate for the Mach number drop through the shock itself at $M = 1.075$. Thus, it appears that if a shock solution had been sought at a lower Mach number than 1.075, there would have been a rapid rise in speed along the wall which would have left a supersonic stream moving faster than the original stream. The present investigation needs extension at this point if questions concerning the first appearance of a shock wave are to be answered.

It thus appears that this report takes a step in the direction of clarifying the so-called critical conditions associated with the first appearance of shock waves but falls far short of an adequate explanation.

It appears that not only is the perfect fluid without shocks an insufficient mathematical theory to cover the practical phenomena arising in connection with the flow of compressible fluids but that even the extended theory which includes compression shock discontinuities, as in this report, is not adequate to describe the facts properly. It is probable that a sufficiently general mathematical theory (and presumably a fluid with friction would provide such) could give smooth transitions from one type of solution to another. There is, however, no reason to assume that such solutions would be either unique or stable.

It may be argued that the sudden jump from one type of solution to another, as required by the present theory, does not contradict experimental observations. True. However, consider the case in which Taylor's limiting solution occurs for a passage in which the velocity at no point has yet risen to as high a value as $M = 1.07$. In this case no shock waves can arise at all if a discontinuous increase of velocity at the wall is considered objectionable. The present theory (perfect fluid with shocks) is not adequate to cover all cases but must be extended.

Figures 19 and 21 should be compared with figure 1. It is seen that the one-dimensional theory has been modified considerably and has been modified in different ways for the nozzle axis and for the nozzle wall.

The flow through the nozzle is plotted against pressure at various points in figures 24, 25, and 26. The reason for the differences in appearance of these figures can be understood by comparison with figures 4 through 16, 19, and 21. The importance of these differences follows if it is considered that nozzle experiments are usually performed by regulating the pressure in a large tank into which the gas discharges or by regulating the pressure at a small hole located somewhere in the nozzle wall. It is quite obvious that there is no guarantee that a single-valued relation exists between the pressure at a given point and the flow through the nozzle. It is quite possible for a decrease in pressure to correspond to a decrease in flow rather than the usual increase in flow. In particular, a pressure hole drilled at certain points in a nozzle may read a given value for as many as three different flows. It may well be that some of these are more stable than others, and therefore experimental difficulties and anomalies might well arise in nozzle experiments. A few additional results of interest are shown in figures 27 and 28.

In figure 27 the distribution of rotation in the nozzle is shown for the solution of figure 13. This rotation is far from negligible, particularly as the shock wave moves downstream and becomes stronger. This rotation is such that it will require the stream to separate from the wall sufficiently far downstream from the nozzle throat. For the perfect fluid considered here, the rotation once produced cannot be destroyed. Thus far downstream from the nozzle throat where the velocity (without rotation) would approach zero, it cannot now do so since the rotation does not decrease. The stream function is to be considered as a surface plotted over the region of space through which the fluid flows. This surface will have the same shape as a soap film stretched over a hole the shape of the domain and loaded with a pressure proportional to the fluid rotation at the corresponding point. If such a film were made for the present nozzle, the soap film would be steepest at the throat and become flatter and flatter on receding from the throat either upstream or downstream. Thus the fluid velocity would be greatest at the throat and approach zero at infinity. If there is rotation, however, the soap film would be loaded. Since the rotation cannot decrease, the loading does not decrease away from the throat and hence the soap film, instead of becoming flatter and flatter, is bulged by the load. If the slope of the soap film is again interpreted as fluid velocity, the fluid will be moving away from the throat on one side of the bulge and toward the throat on the other. Where the bulge first starts, there would be the separation point in the nozzle. The consequences of this separation were not investigated. While this analogy is strictly correct for incompressible fluids only, it shows clearly the problem involved.

In figure 28 the variation in entropy behind the shock waves is shown for all of the solutions with shocks. Since entropy is a function of the stream function only for a particular solution, such a composite figure is possible (such a figure is not possible for the rotation which is a function of pressure as well as entropy gradient). By a reference to the computation curves of the earlier report (reference 7), it is obvious that this change in entropy causes a very considerable alteration of the properties of the fluid. It is for this reason that the pairs of figures, 18, 19, and 20, 21, show considerable differences. (For constant entropy, $p = f(M)$, and these figures would differ only by an ordinate scale change.)

In figure 29 the shock waves for all the solutions are assembled for comparison. It is clear how the shock waves arise near the wall, grow and move downstream.

EFFECTS OF FRICTION

Figure 30 shows a series of photographs of the flow through a hyperbolic nozzle taken in a high-speed wind tunnel at Harvard University. It is not surprising that this flow in no case looks like the predicted flow. The relatively small radius of curvature at the throat of the nozzle investigated makes it impossible for a real gas with friction to follow the walls. Since for low velocity a jet separating from both walls is not very stable, the stream usually separated from one wall and passed along the other (flow nonsymmetrical about axis of nozzle). As soon as shock waves of reasonable magnitude appeared, the stream separated from both sides and passed out as a free jet. Thus, there will have to be included in any complete investigation the effects of friction on the modification of the effective boundary shape by the boundary layer, which modification will eventually have to include flow separation which at the present cannot be satisfactorily predicted; and also the boundary layer will introduce very considerable changes in the partial shock waves which appear and consequently will greatly affect the pressure and velocity distributions along the wall near the throat of the nozzle. Such friction effects will, it is reasonably certain, always lead to flow separation at least locally between the end of a shock wave and the wall. Two other effects which might be worthy of note, although not coming directly under the heading of friction, are (1) moisture in the air and (2) heat transfer. It is quite probable that the first shock wave encountered by the stream in the photographs of figure 30 is closely connected with the moisture in the atmosphere as changes in form of this "throat shock" occur with changes of atmospheric moisture.

The consideration that the nozzle is not thermally connected to any source or sink of heat (generally not true) is not a guarantee that no heat transfer to the air stream takes place. Since the temperature in the boundary layer of a gas with Prandtl number other than $Pr = 1$ would not be constant, the nozzle to be in equilibrium with the gas would have a varying wall temperature along the nozzle length. For a metal nozzle this would necessitate a considerable flow of heat from one portion of the nozzle to another and hence from one portion of the gas stream to another. It is not likely that this effect is ever very large but it should not be forgotten completely since, in some cases, it might be significant.

CONCLUSIONS

The two-dimensional flow of a frictionless, adiabatic, perfect gas through a hyperbolic nozzle follows very closely that to be expected from the investigations of Taylor (reference 3) as long as no shock waves appear. A symmetrical supersonic region appears near the wall at the throat for a sufficiently high flow through the nozzle. There is a greatest flow above which this type of flow no longer exists.

In spite of attempts to determine exactly what it was that caused the symmetrical solutions to cease existing it could only be noted that as the maximum velocity got higher, the residuals (local fluid rotation) became more and more difficult to dispose of. When it became absolutely impossible to dispose of the rotation (a state of affairs that is sure to remain uncertain in a finite computation effort), shock waves arise which greatly alter conditions and incidently produce some rotation, thus permitting a solution to be found.

The solutions presented in this report constitute a story of the growth of the flow pattern inside of a nozzle from zero velocity to the highest attainable velocity. This flow picture is a good first approximation to what really happens in a two-dimensional nozzle as long as the real flow through the nozzle is free from flow separation. Further accuracy of prediction of what happens in a nozzle can be attained only by using a more complicated fluid continuum which at least has the additional property of friction.

Critical (greatest) flow through a nozzle is not reached until the shock wave first extends all the way across the nozzle passage. During the growth of the partial shocks, however, the flow changes only 1 percent. The greatest flow is 0.7 percent less than the theoretical maximum that would be obtained if the $M = 1$ line extended across the nozzle at the throat.

Harvard University,
Cambridge, Mass., February 10, 1945.

APPENDIX I

SOLUTIONS WITH COMPRESSION SHOCKS

In a previous report (reference 7) a brief description was given of the method of fitting compression shocks into the numerical solution. This method has been further perfected and is presented here.

In the transformed (ξ,η) plane, the streamlines, ψ = constant, almost coincide with the η constant lines when the shock waves are nearly normal. This circumstance greatly simplifies the resulting formulas, so that the derivation will be carried out with these assumptions. Figure 31 shows a streamline crossing a shock wave from the supersonic, b, region to the subsonic, a, region. The obliquity, θ_w, of a shock is given by computation curve 5 of reference 7 in terms of the Mach number of the approaching stream and the deflection angle φ. This deflection angle can be computed from the residuals at points 1 and 2 as follows. The streamline makes an angle α with the ξ axis given by

$$\tan \alpha = \left(\frac{\partial \eta}{\partial \xi}\right)_\psi = -\frac{\psi_\xi}{\psi_\eta} \tag{4}$$

Thus

$$\varphi = \alpha_a - \alpha_b \approx \frac{\psi_{\xi_b}}{\psi_{\eta_b}} - \frac{\psi_{\xi_a}}{\psi_{\eta_a}} \approx \frac{\psi_{\xi_b} - \psi_{\xi_a}}{\psi_\eta} \tag{5}$$

where the last form is obtained by neglecting the very small difference between ψ_{η_b} and ψ_{η_a}.

Now, observe that if the shock wave had not been present there would have been a "supersonic" value of ψ_{2_b} at point 2 which would have made the residual at point 1 equal to zero. If, however, the value of ψ_{2_a} from the subsonic solution is used in computing the residual Q_1, it will have the value

$$Q_1 = \psi_2 - \psi_{2_b} = \psi_2 - \psi_1 - \psi_{\xi_b}\,\delta \tag{6}$$

or

$$\psi_{\xi_b} = \frac{\psi_2 - \psi_1 - Q_1}{\delta} \tag{7}$$

Similarly

$$\psi_{\xi_a} = \frac{\psi_2 - \psi_1 + Q_2}{\delta} \tag{8}$$

Substitute these into equation (5)

$$\varphi = -\frac{Q_1 + Q_2}{\delta\psi_\eta} = -2\,\frac{Q_1 + Q_2}{\psi_4 - \psi_5} \tag{9}$$

Another relation to be satisfied by the shock wave is obtained by observing that the value of ψ does not change across the shock. Thus

$$\psi_1 + \epsilon\delta\psi_{\xi_b} = \psi_2 - (1 - \epsilon)\,\delta\psi_{\xi_a} \tag{10}$$

from which

$$\epsilon = \frac{\psi_2 - \psi_1 - \delta\,\psi_{\xi_a}}{\delta(\psi_{\xi_b} - \psi_{\xi_a})} \tag{11}$$

Again using the relations (7) and (8)

$$\epsilon = \frac{Q_2}{Q_1 + Q_2} \tag{12}$$

The shock wave divides the distance between net points inversely as the residuals.

Finally, a shock wave as treated in this report, is assumed to be continuous, not branched, and ending either at the wall or where $M = 1$.

The technique of solution, then, is to attempt to eliminate all residuals. Failing this, an attempt is made to accumulate all residuals along some line among the points. In

the present work it was always fairly obvious where the shock would be by observing the trend of solutions. Furthermore, by observing the sign of the rotation term that is needed after the shock to balance the decrease of the density term, it was fairly obvious which way to bend the shock. Hence, early in the course of solution, it was possible to sketch in a likely shock wave and with equations (9) and (12) to compute the required residuals at points on both sides.

Now as the solution progresses, and residuals are moved to the tentative shock position, the shock wave angle and position (by continuity of shock line these are not independent) are gradually altered. Specific instructions at this point cannot be given but it is worth observing that for any initial Mach number there is a maximum possible deflection angle and that for shock waves in a stream near $M = 1$, the maximum permissible deflection is very small. Hence care must be exercised during solution to avoid exceeding the maximum permissible sum of residues as given by equation (9) with the maximum φ.

The formulas of this appendix were derived after making assumptions about the streamlines and shock waves ($\tan \alpha_a \approx \alpha_a$, $\tan \alpha_b \approx \alpha_b$). As a solution nears completion, these assumptions can be checked. If they are not met with sufficient accuracy, more elaborate formulas must be derived using essentially the same methods as the above-mentioned.

APPENDIX II

THE STREAMLINE CURVATURE JUMP ACROSS NORMAL SHOCK WAVES

Let a streamline pass through a shock wave as in figure 32, and suffer a jump in radius of curvature from R_b to R_a. Assume the stream approaching the shock wave is a perfect gas with uniform stagnation state. The approach flow will then be irrotational.

The momentum condition applied normal to the streamlines gives

$$\frac{\partial p}{\partial r} = \frac{\rho q^2}{r} \tag{13}$$

for each side of the shock wave. Hence, by division,

$$\frac{R_b}{R_a} = \frac{q_b}{q_a}\left(\frac{\partial p_a}{\partial p_b}\right)_s \tag{14}$$

where the subscript s denotes that the derivative is to be evaluated along the shock wave.

The change in pressure across the shock is given by the momentum equation as

$$p_a = p_b + \rho_b q_b^2 - \rho_a q_a^2 = p_b + \rho_b(q_b^2 - q_a q_b) \tag{15}$$

in view of the continuity condition $\rho_b q_b = \rho_a q_a$.

Before eliminating p_a between equations (14) and (15), it is well to note Prandtl's relation

$$q_a q_b = q_{cr}^2 = \frac{2}{\gamma - 1} a_b^2 + \frac{\gamma - 1}{\gamma + 1} q_b^2 \tag{16}$$

where q_{cr}^2 is a constant because of the assumed constant stagnation state of the approach stream.

Now by equation (14)

$$\frac{R_b}{R_a} = \frac{q_b^2}{q_{cr}^2}\left(1 + \frac{\partial p_b(q_b^2 - q_{cr}^2)}{\partial p_b}\right) \tag{17}$$

where the subscript s is dropped, as the derivative now depends only upon the approach Mach number. In fact R_b/R_a depends only upon the approach Mach number.

Carry out the differentiation indicated in equation (19) and note that $a^2 = \frac{\partial p}{\partial \rho}$ and $M = \frac{q}{a}$. There results

$$\frac{R_b}{R_a} = \frac{q_b^2}{q_{cr}^2}\left\{1 + \frac{q_b^2 - q_{cr}^2}{a_b^2} + \rho_b \frac{\partial q_b^2}{\partial p_b}\right\} \tag{18}$$

The remaining derivative term is found to have the value -2 by using the momentum equation along the streamlines

$$q\ d\ q + \frac{dp}{\rho} = 0 \tag{19}$$

Thus

$$\frac{R_b}{R_a} = \frac{q_b^2}{q_{cr}^2}\left(M^2 - 1\right) - M^2 \tag{20}$$

By eliminating q_{cr}^2 from equations (16) and (20), there is obtained finally

$$\frac{R_b}{R_a} = \frac{M^2}{1 + \frac{\gamma - 1}{2} M^2}\left[M^2 - \frac{\gamma + 3}{2}\right] \tag{21}$$

The ratio of curvature radii varies from -1 at $M = 1$, through 0 at $M = \sqrt{\frac{\gamma + 3}{2}}$ (= 1.482 for $\gamma = 1.40$), through +1 at $M = 1.66$ for $\gamma = 1.40$, and $\longrightarrow \infty$ as $M \longrightarrow \infty$. The curve is shown as computation curve (fig. 22). The Mach number at which no change in curvature occurs across a shock wave is given by

$$M = \left\{\frac{\gamma + 1}{2} + \left[\left(\frac{\gamma + 1}{2}\right)^2 + 1\right]^{\frac{1}{2}}\right\}^{\frac{1}{2}}$$

APPENDIX III

ADDITIONAL REMARKS ON THE NUMERICAL SOLUTION OF SUPERSONIC REGIONS

There was no definite procedure specified in the previous report (reference 7) by which solutions in supersonic regions could be obtained. It is still impossible to write any rigid instructions that are sure to work. This is a general difficulty as Fox and Southwell (reference 9) state that their iteration method diverged after reaching a minimum value.

The residuals in the solutions could be reduced considerably by the following procedure:

1. Obtain a rough solution using q^* constant as explained in reference 7.

2. Move residuals around somewhat in an attempt to improve the solution. During this process, draw q^* versus η curves to see that they are smooth. This is especially important for the evaluation of the properties at the nozzle wall.

3. Use a finer net making a first estimate of net values by using a q^* variation as already found for the coarse net.

Some trouble may be experienced in interpolating to a finer net in regions were $M \approx 1$. The variation of q_i from point to point may be such that, on interpolating, the ψ gradient exceeds the maximum possible value; or if the gradient is held down to its maximum permissible value, then the resulting streamline with the fine net may differ considerably from the corresponding streamline on the coarse net. This difficulty could be avoided by using at each net point not the q_i for that point, but an average q_i for that point and two points on each side of it on the next finer net. Using an average from a still finer net was found to offer no additional advantage. The five q_i values (one at desired point and two on each side on finer net) were weighted 1, 2, 2, 2, 1 which gives approximately the area in the

region $\pm\delta$ on each side of the desired point. A few other averages were tried without noticeable benefit. In particular, since the mass flow is almost constant near $M = 1$, it can be shown that a harmonic mean should be taken but the resulting "effective" q_i was not appreciably different from the average as above-mentioned.

REFERENCES

1. Stodola, A.: Steam and Gas Turbines. McGraw-Hill Book Co., Inc., 1927.

2. Anon.: Theoretical Studies on the Flow through Nozzles and Related Problems. AMP Rep. 82.1 R, NDRC, Applied Mathematics Group, New York Univ., April 1944.

3. Taylor, G. I.: The Flow of Air at High Speeds past Curved Surfaces. R. & M. No. 1381, British A.R.C., 1930.

4. Meyer, T.: Über zweidimensional Bewegungsvorgänge in einem Gas, das mit Überschallgeschweindigkeit strömt. Forschungsarbeiten auf dem gebiete des Ingenieurwesens 62, 1908.

5. Görtler, H.: Zum Übergang von Unterschall - zu Überschallgeschwindigkeiten in Düsen. Z.f.a.M.M., vol. 19, no. 6, Dec. 1939, pp. 325-337; and Gasströmungen mit Übergang von Unterschall - zu Überschallgeschwindigkeiten. Z.f.a.M.M., vol. 20, no. 5, Oct. 1940, pp. 254-262.

6. Ringleb, Friedrich: Exakte Lösungen der Differentialgleichungen einer adiabatischen Gasströmung. Z.f.a.M.M., vol. 20, no. 4, Aug. 1940, pp. 185-198.

7. Emmons, Howard W.: The Numerical Solution of Compressible Fluid Flow Problems. NACA TN No. 932, 1944.

8. Green, J. R., and Southwell, R. V.: Relaxation Methods Applied to Engineering Problems, IX - High-Speed Flow of Compressible Fluid through a Two-Dimensional Nozzle. Phil. Trans. Roy. Soc., ser. A, no. 808, vol. 239, April 1944, pp. 367-386.

9. Fox, L., and Southwell, R. V.: On the Flow of Gas through a Nozzle with Velocities Exceeding the Speed of Sound. Proc. Roy. Soc. London, ser. A, vol. 183, Aug. 10, 1944, pp. 38-54.

10. v. Koppenfels, Werner: Two-Dimensional Potential Flow past a Smooth Wall with Partly Constant Curvature. NACA TM No. 996, 1941.

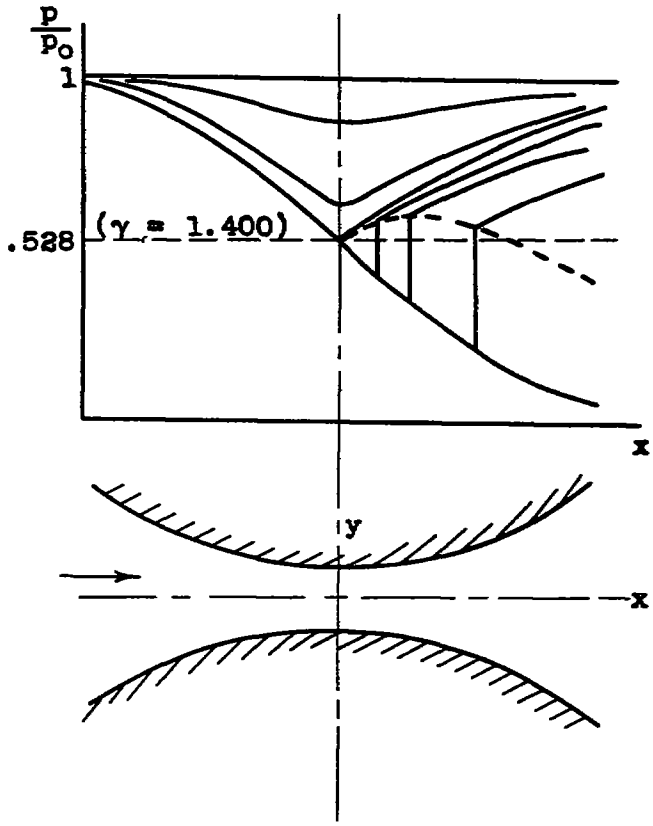

Figure 1.

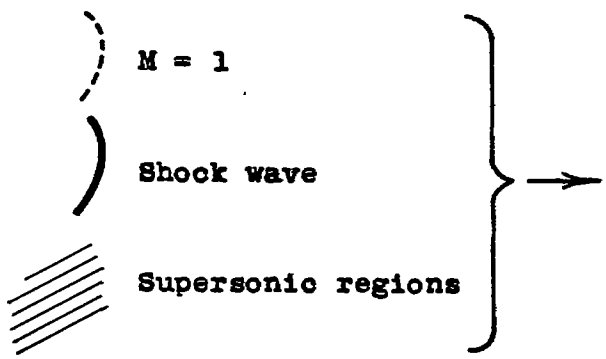

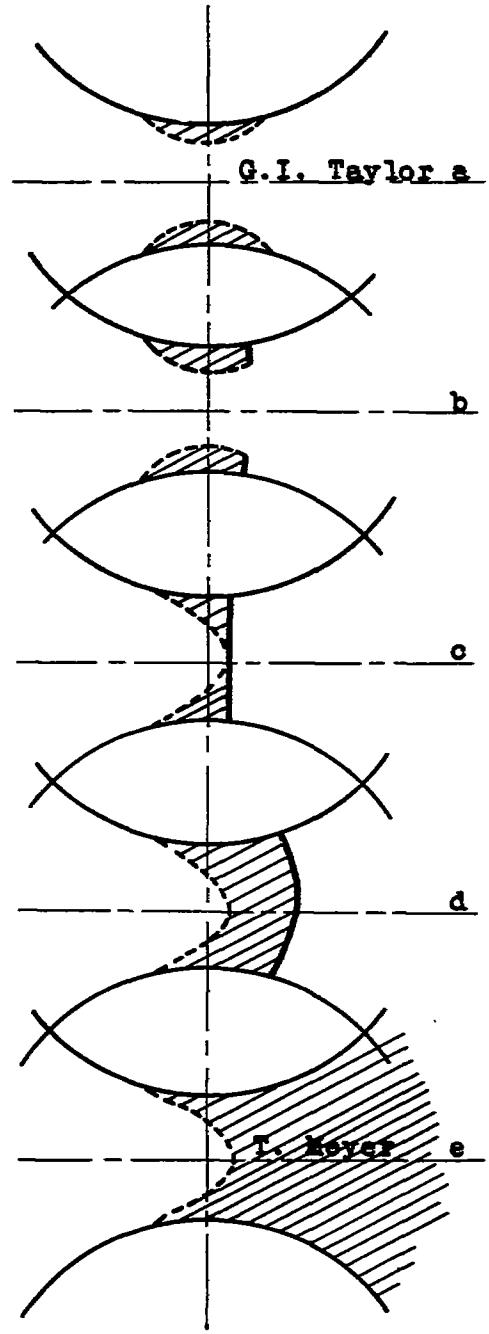

Figure 2.

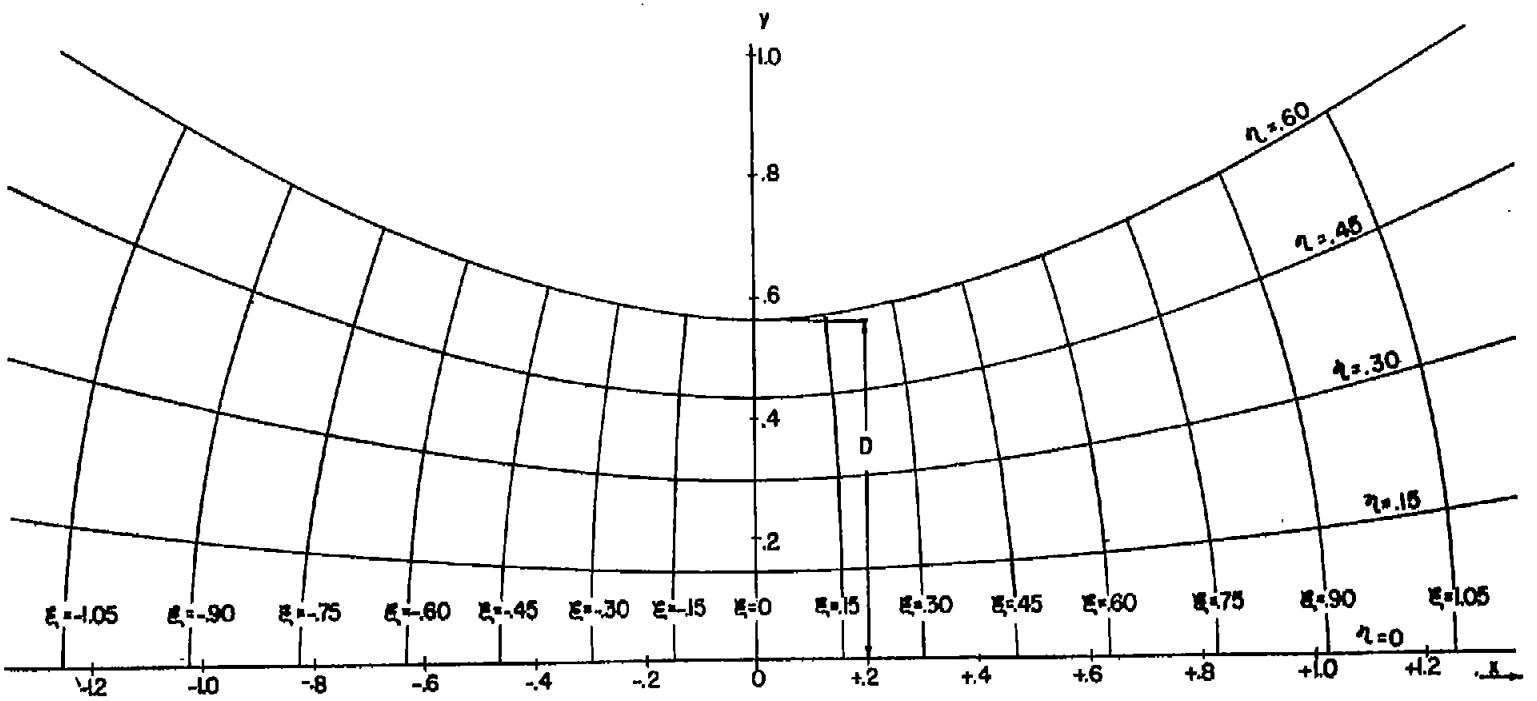

Figure 3.- Flow of compressible fluid in hyperbolic channel; coordinate system used in obtaining solutions.

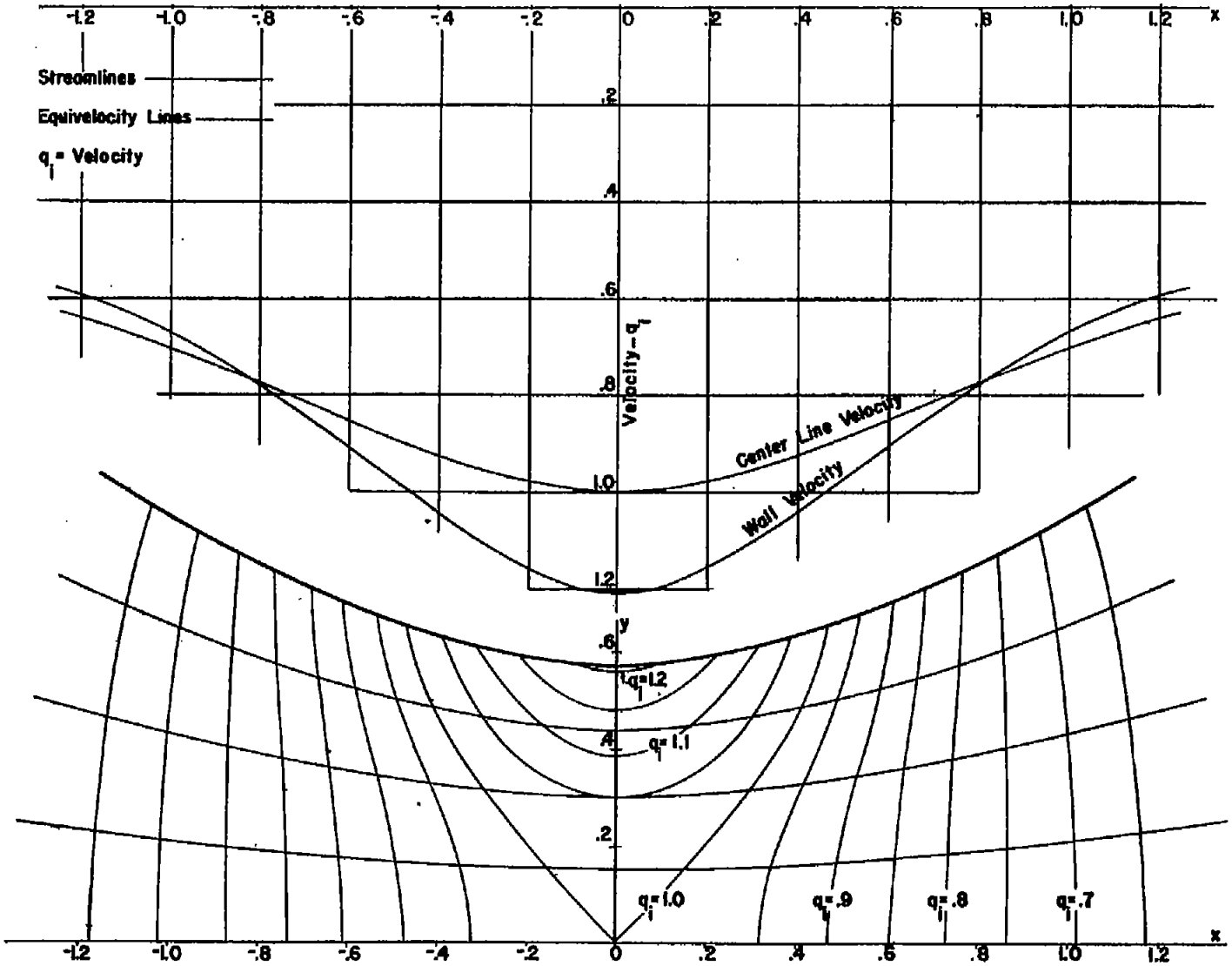

Figure 4.- Flow of incompressible fluid in hyperbolic channel.

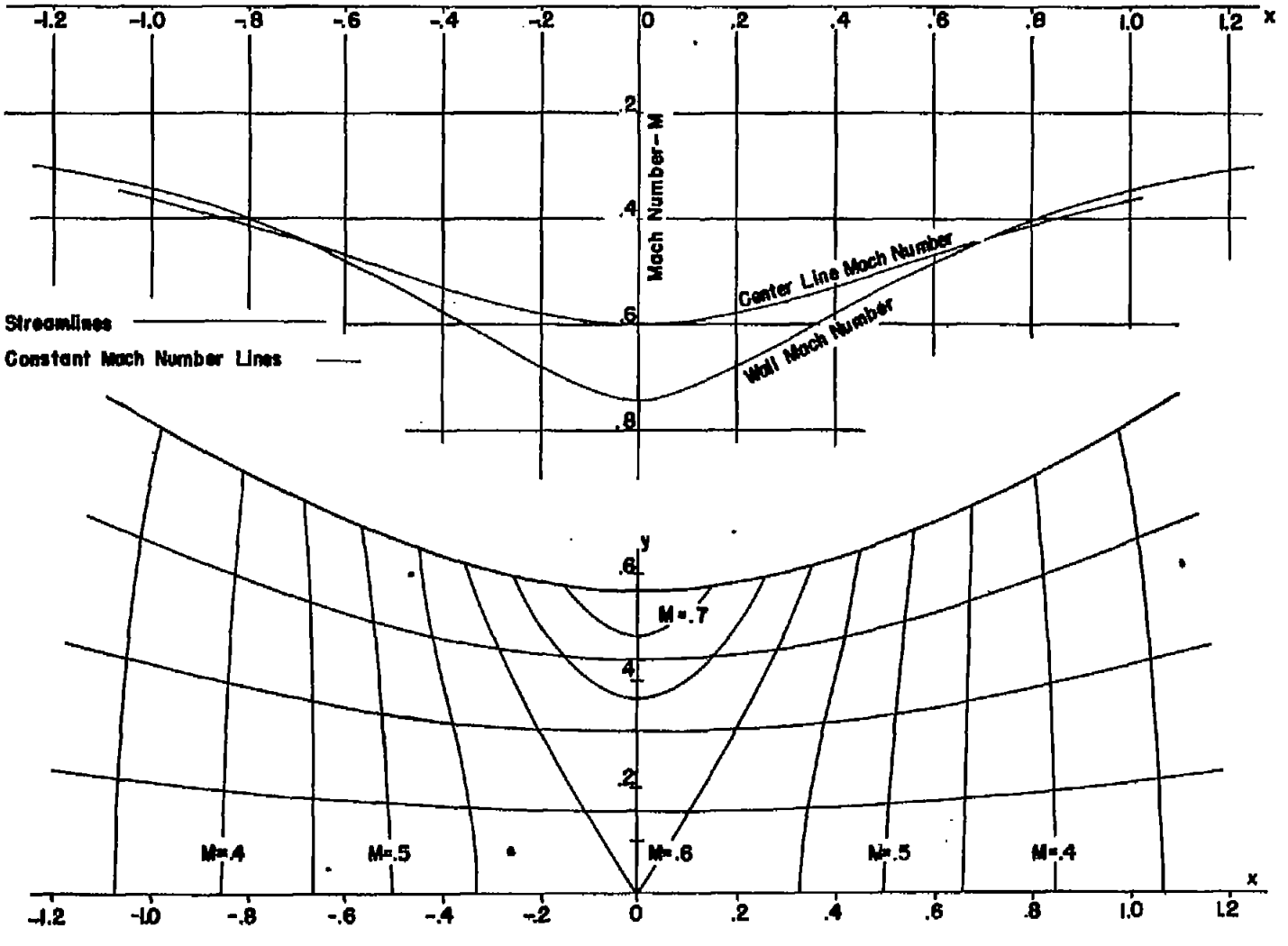

Figure 5.- Flow of compressible fluid in hyperbolic channel. Mach number at center of channel, M = .600.

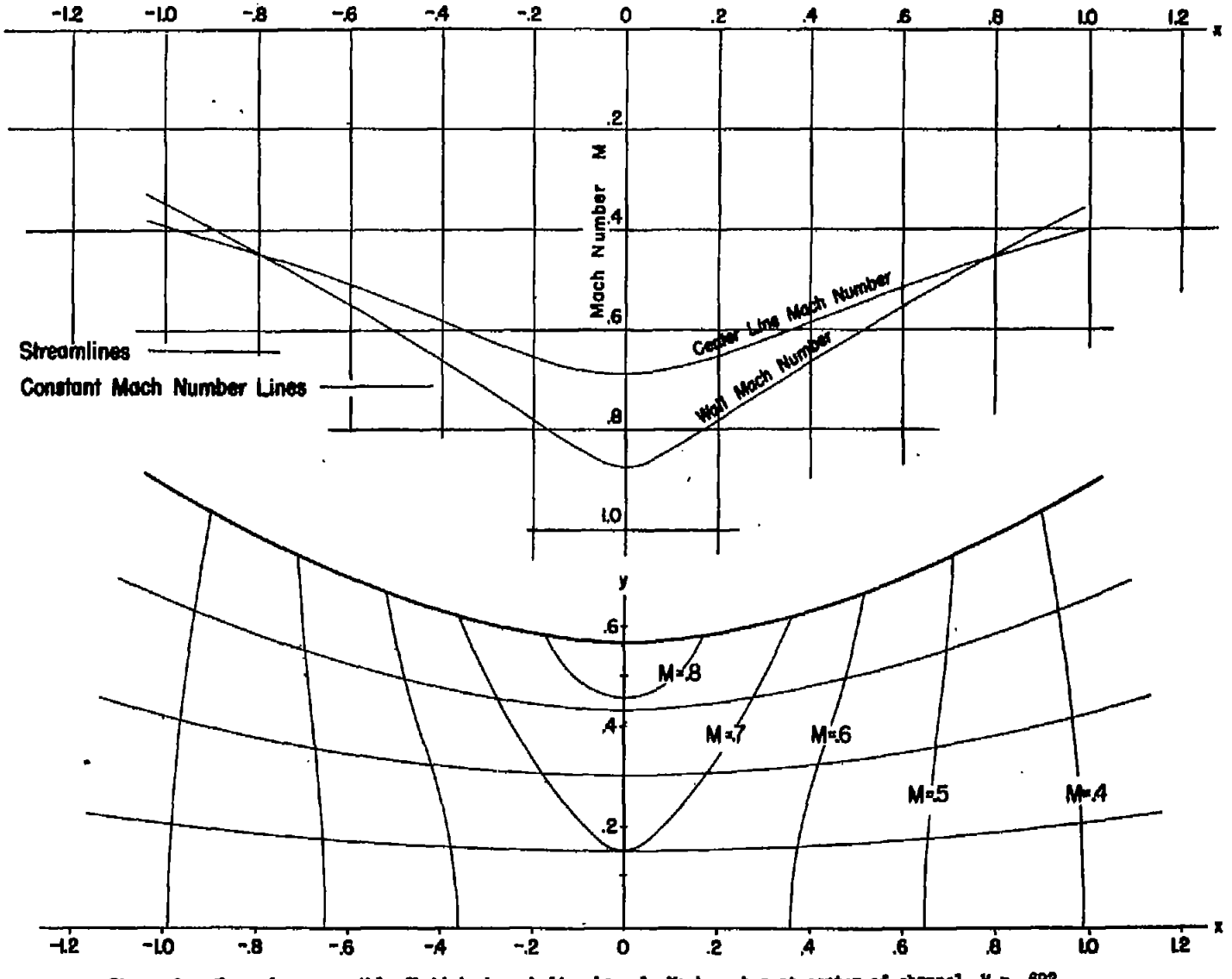

Figure 6.- Flow of compressible fluid in hyperbolic channel. Mach number at center of channel, M = .692.

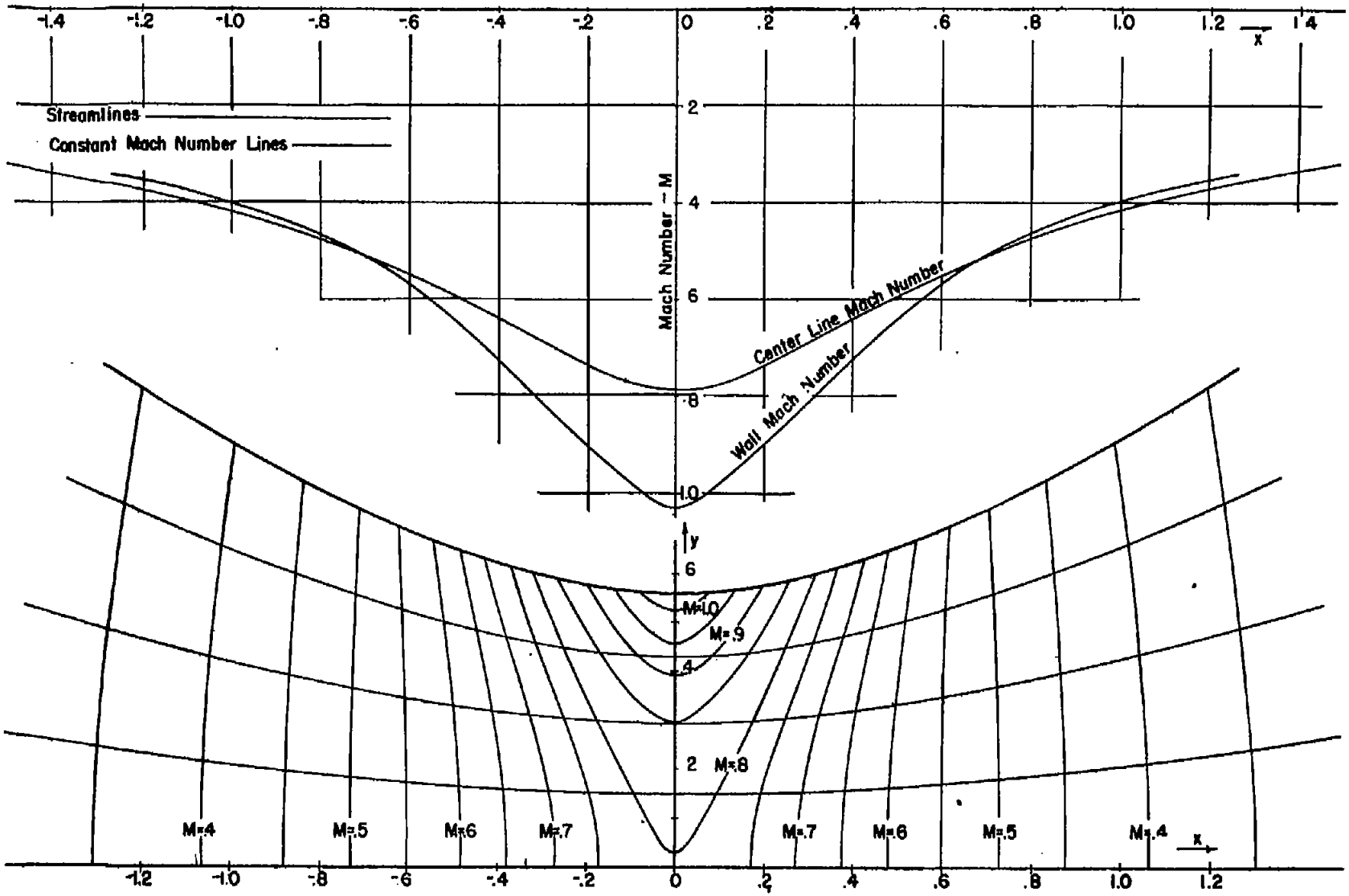

Figure 7.- Flow of compressible fluid in hyperbolic channel. Mach number at center of channel, M = .793.

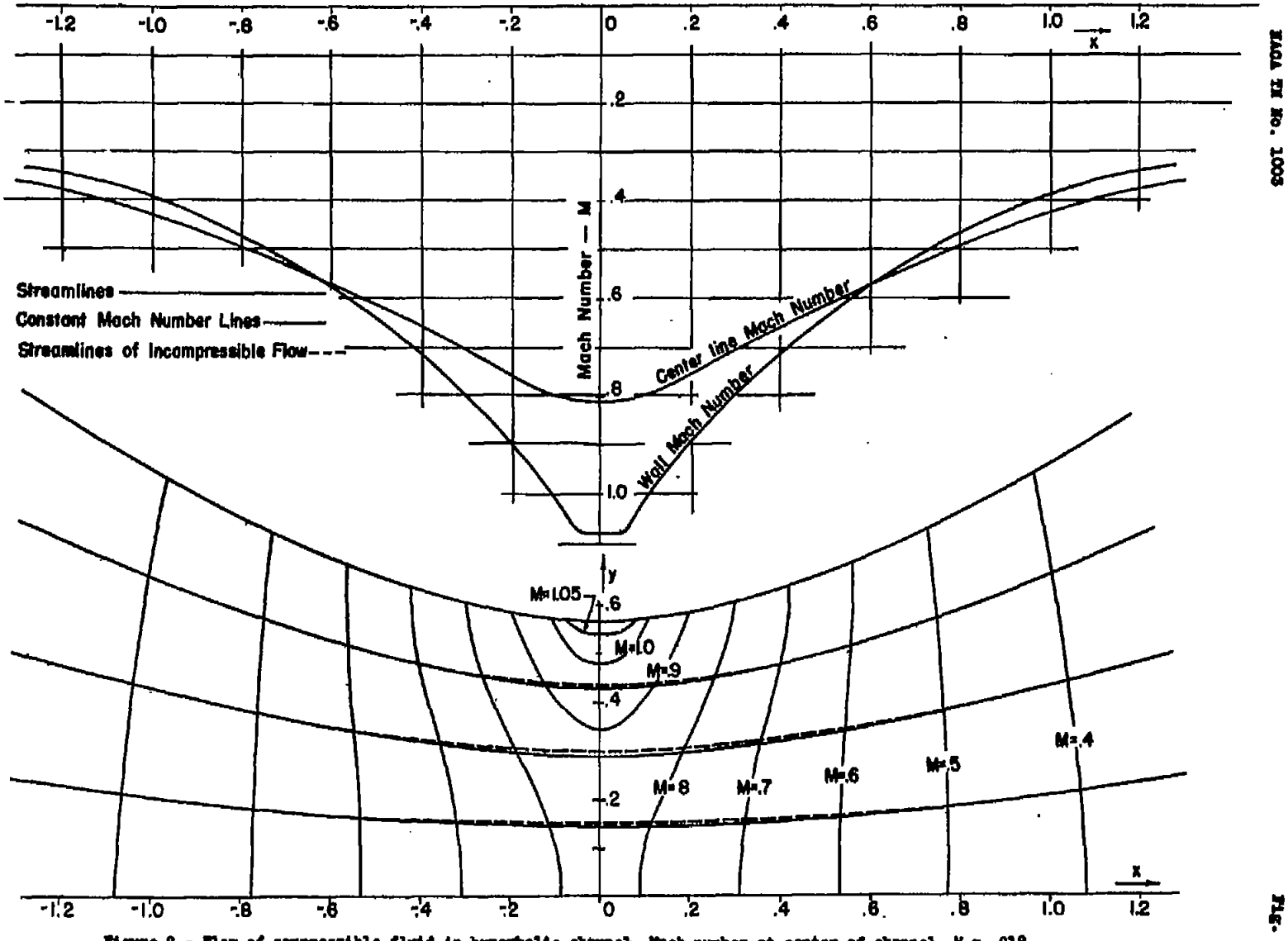

Figure 8.- Flow of compressible fluid in hyperbolic channel. Mach number at center of channel, M = .812.

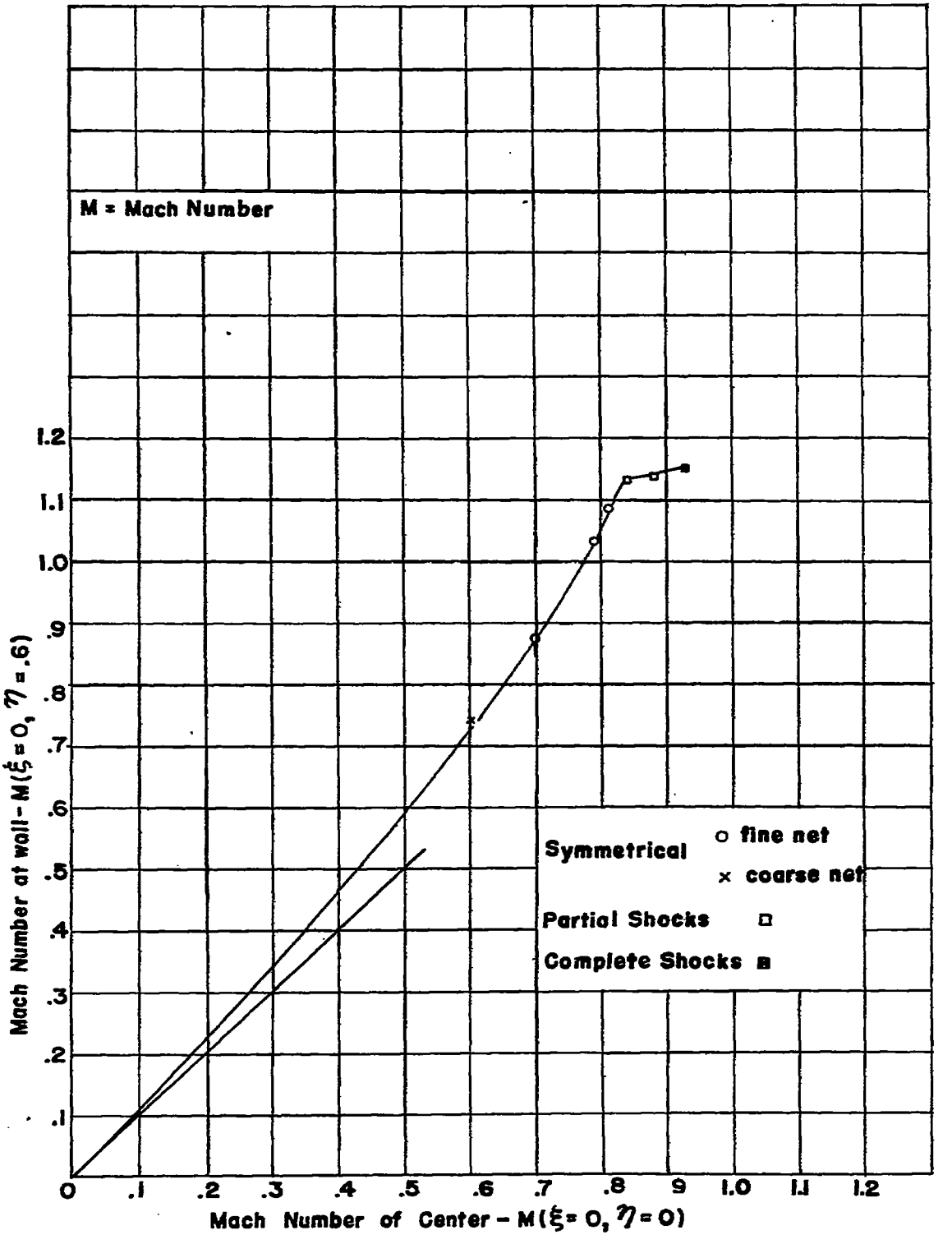

Figure 9.- Relation between M at wall and M at center.

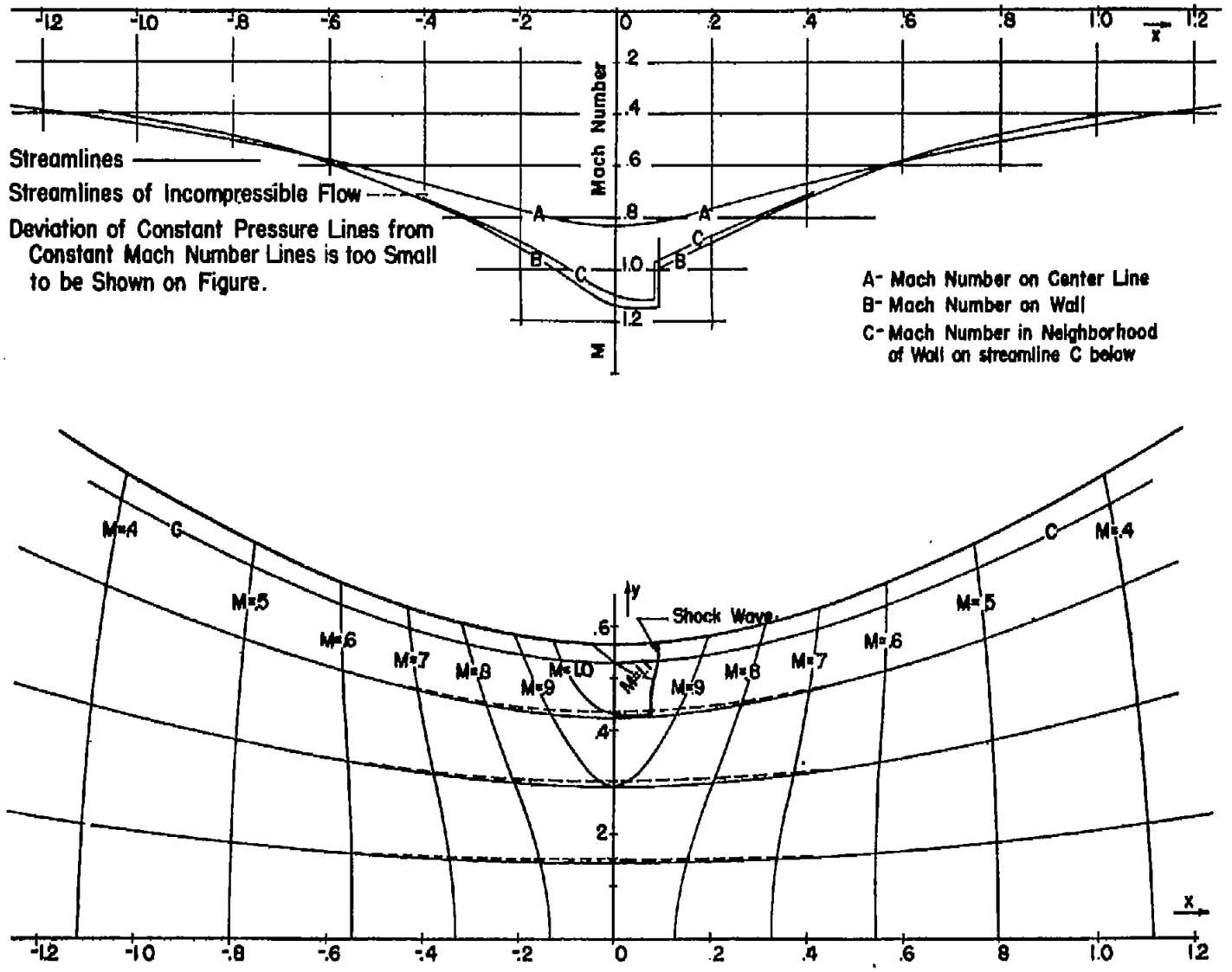

Figure 10.- Flow of compressible fluid in hyperbolic channel. Mach number at center of channel, M = .833.

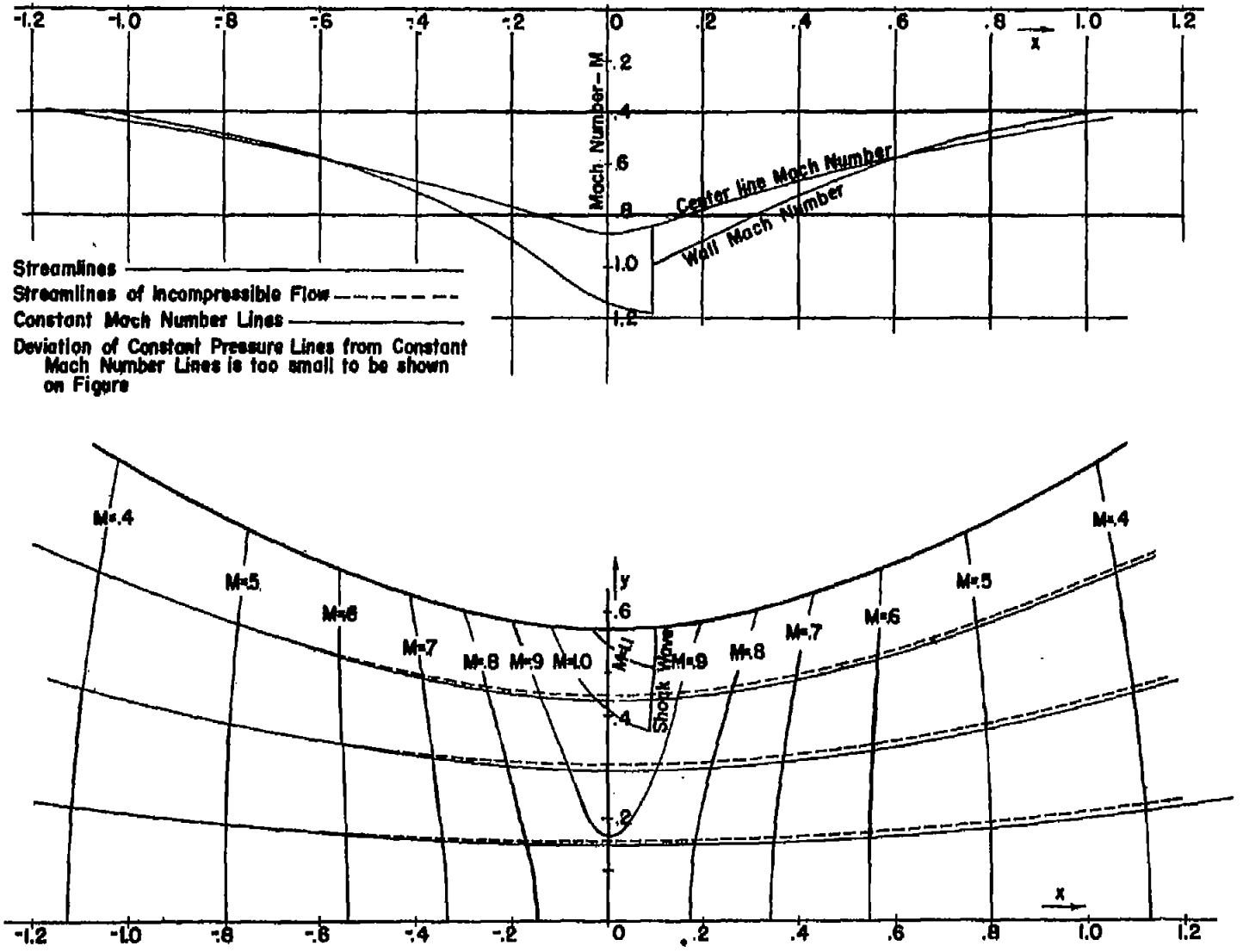

Figure 11.- Flow of compressible fluid in hyperbolic channel. Mach number at center of channel, M = .835.

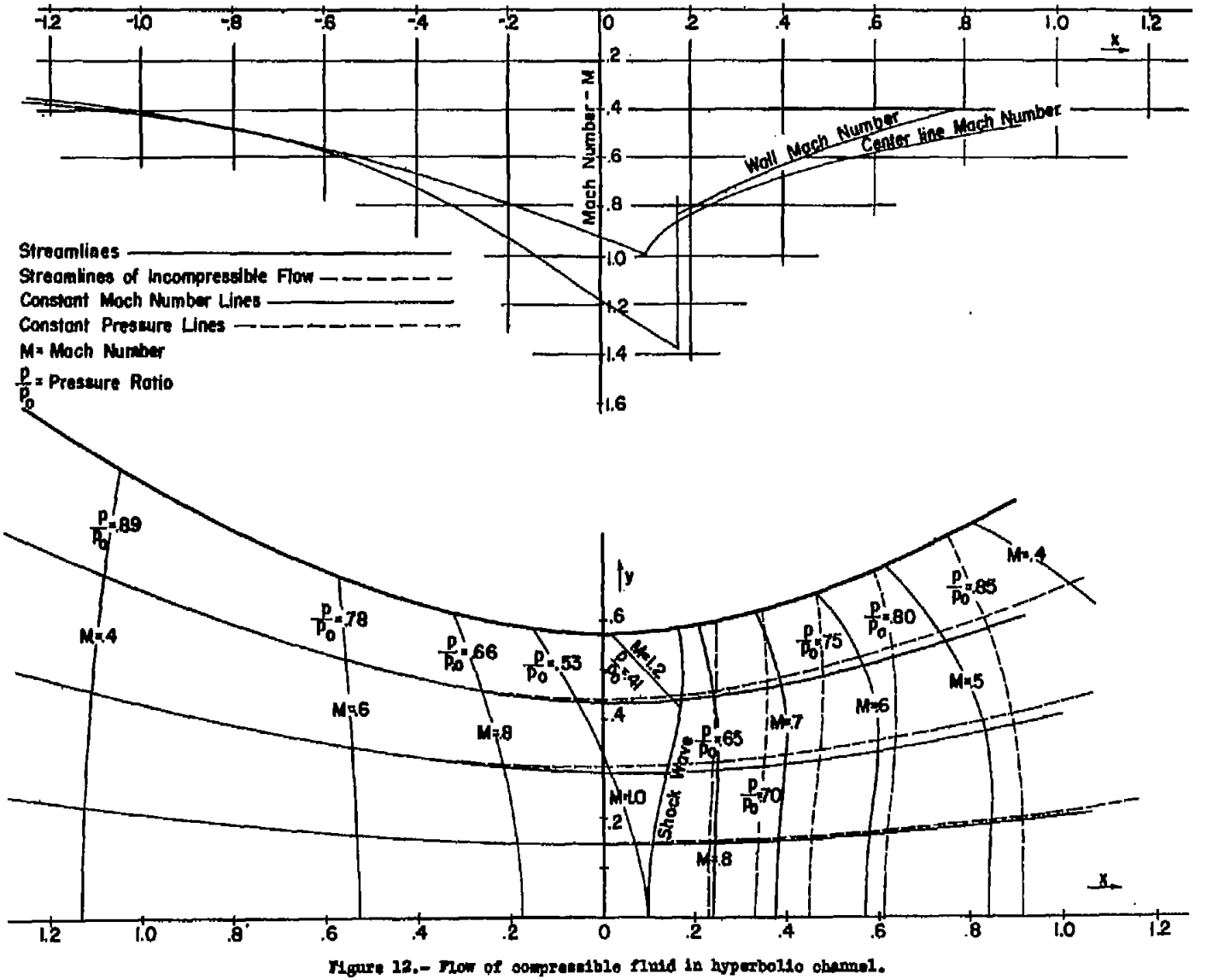

Figure 12.- Flow of compressible fluid in hyperbolic channel.

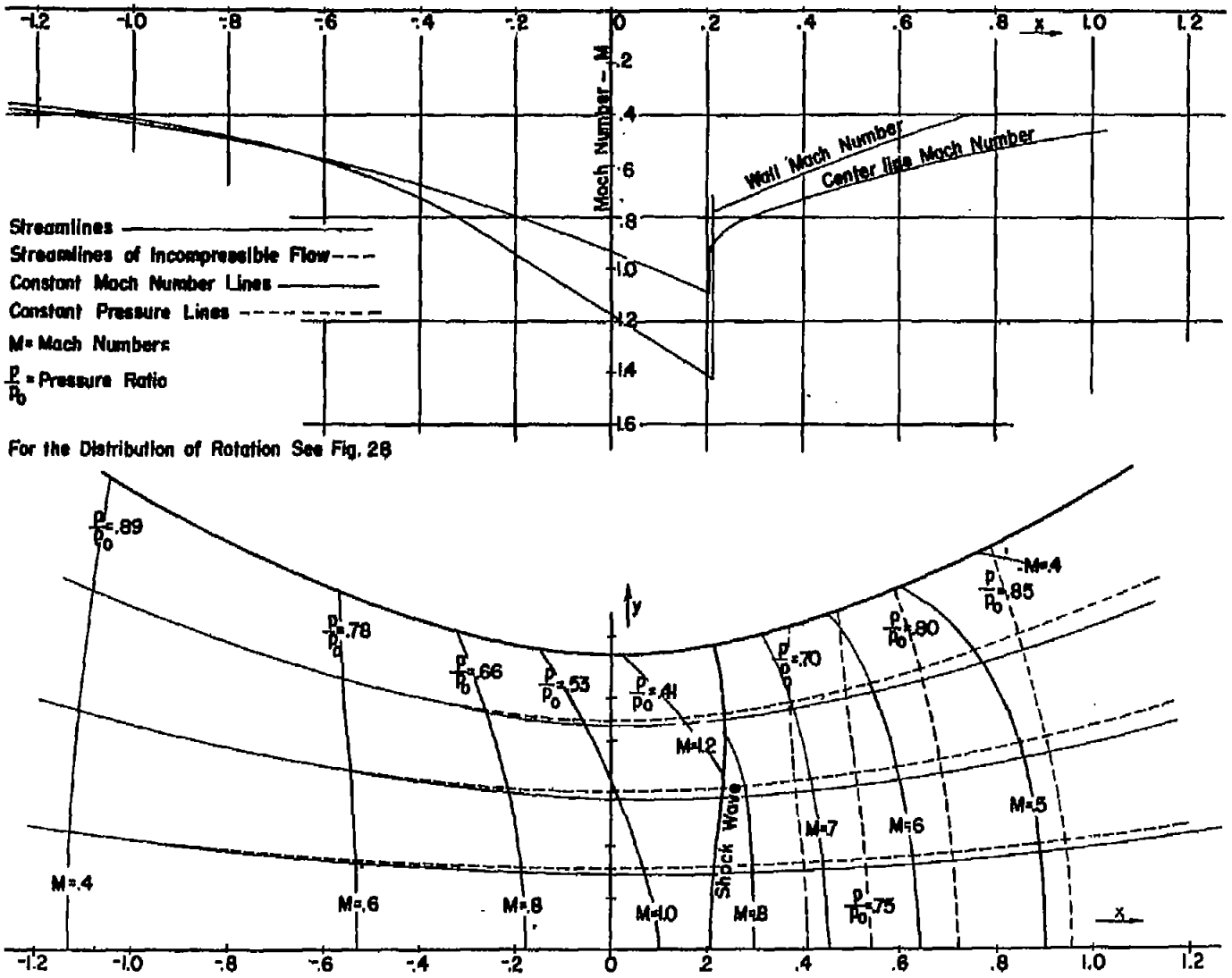

Figure 13.- Flow of compressible fluid in hyperbolic channel.

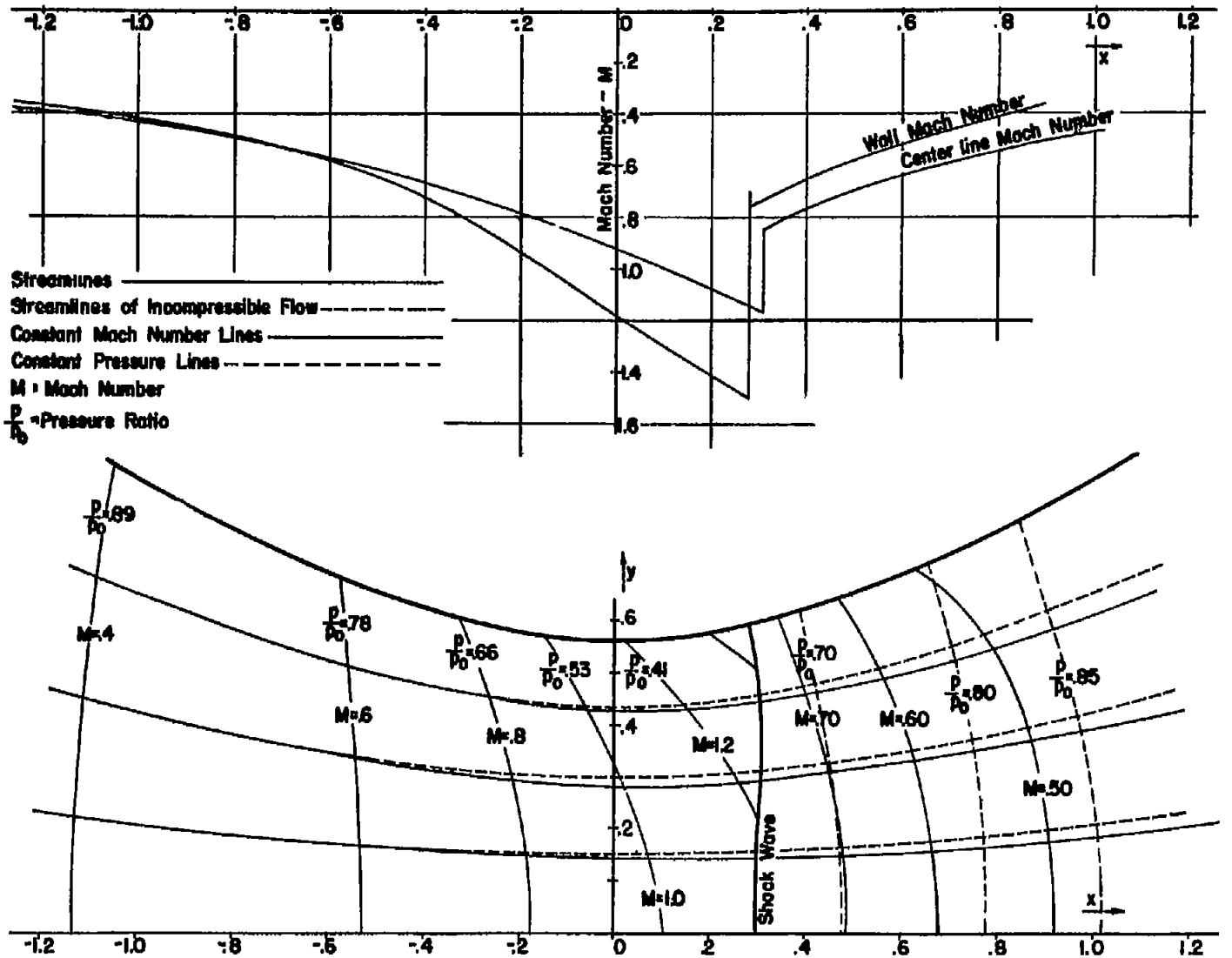

Figure 14.- Flow of compressible fluid in hyperbolic channel.

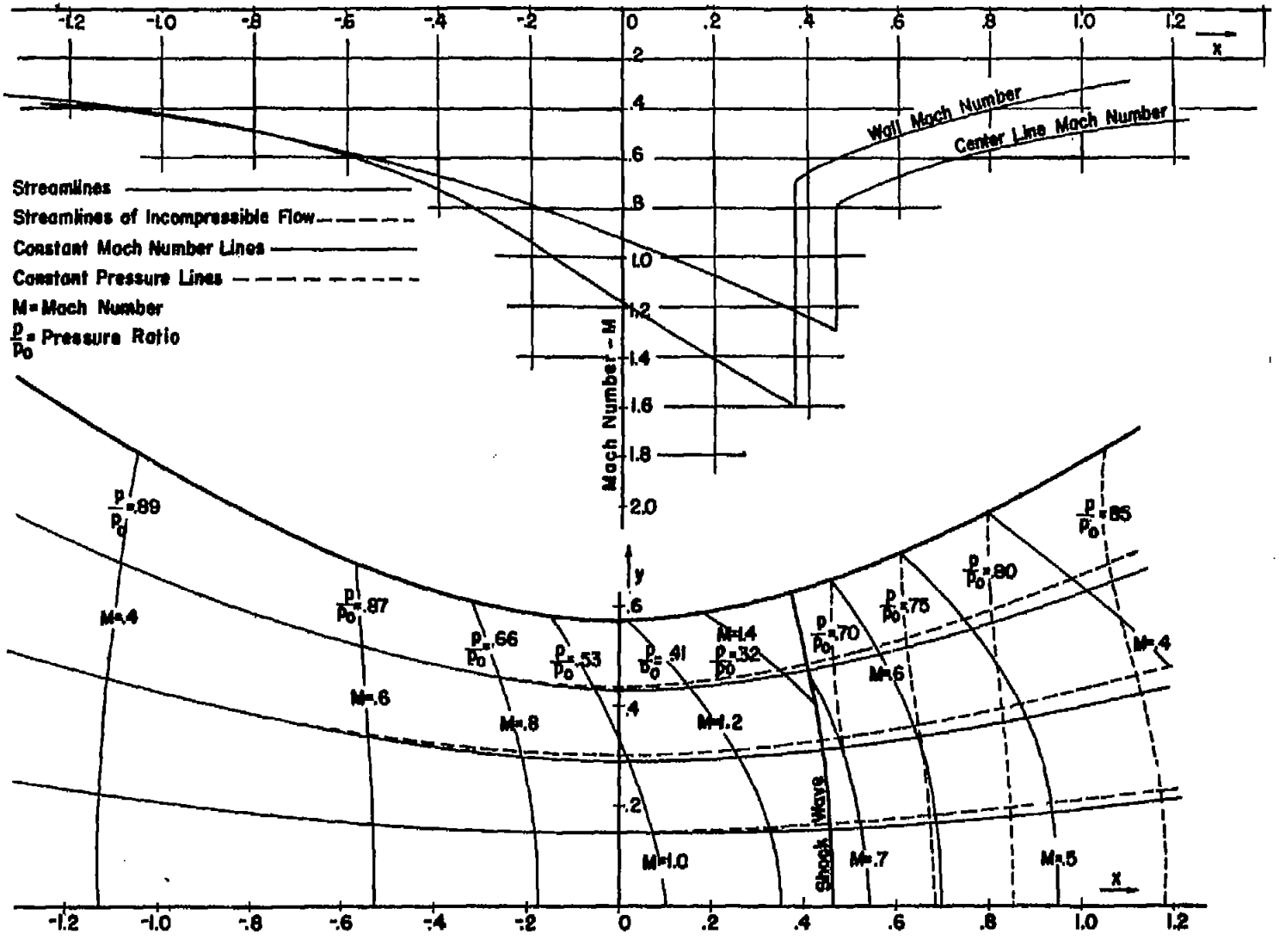

Figure 15.- Flow of compressible fluid in hyperbolic channel.

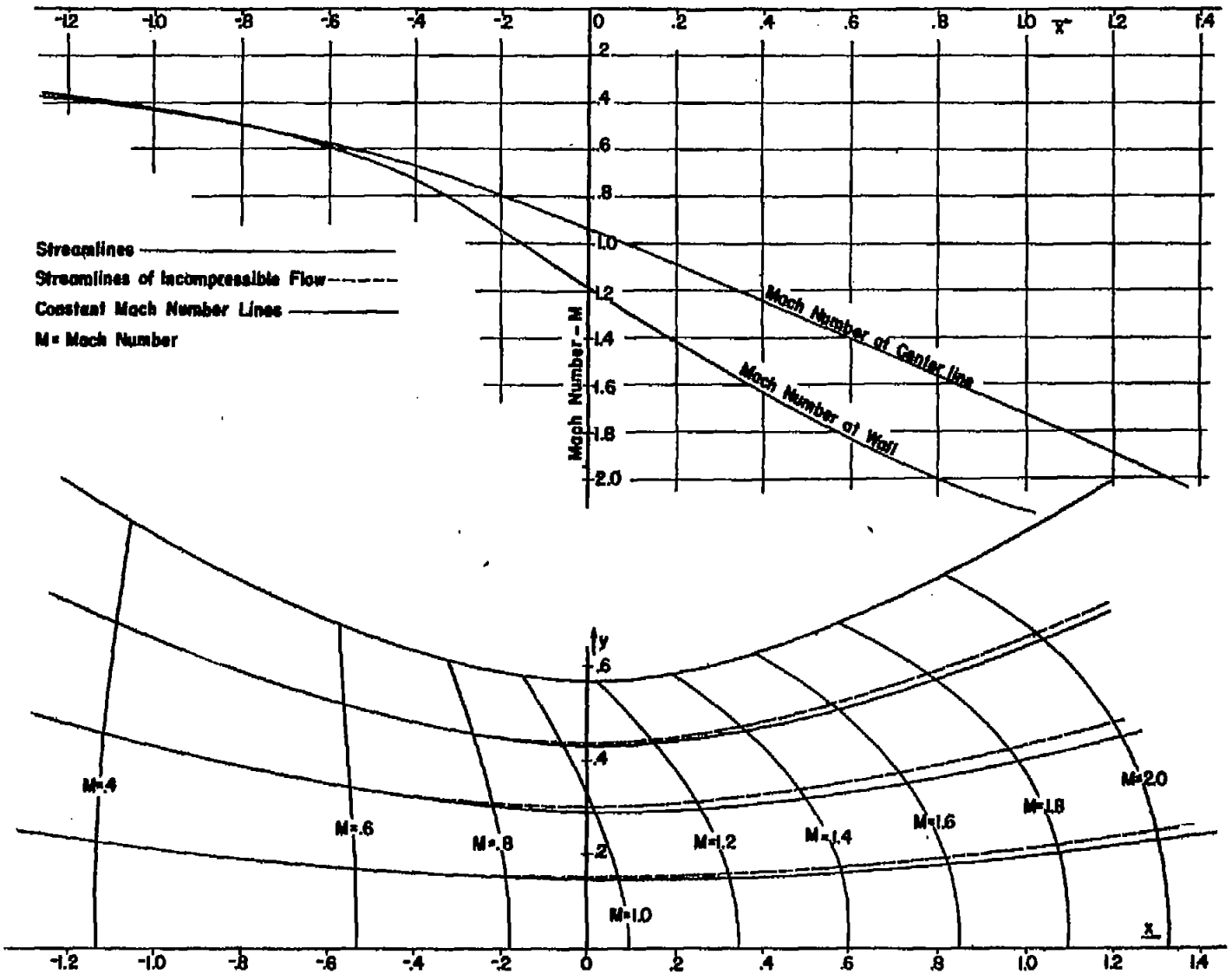

Figure 16.- Flow of compressible fluid in hyperbolic channel.

q ⟶

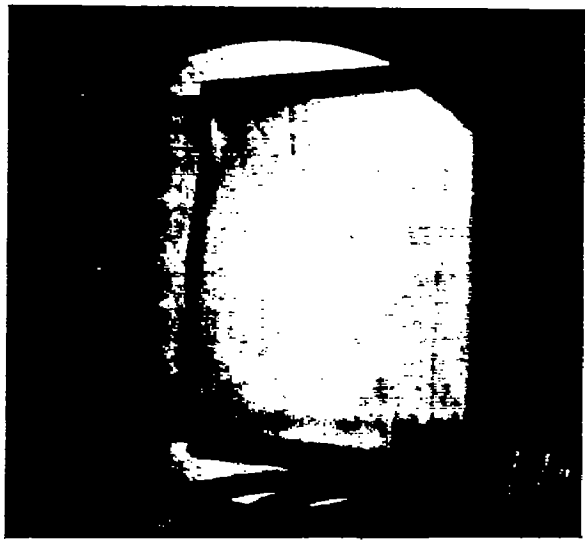

(a) Shock wave at nozzle throat. Exposure 1/10 second.

On attempting to repeat the above experiment the following photograph was obtained.

q ⟶

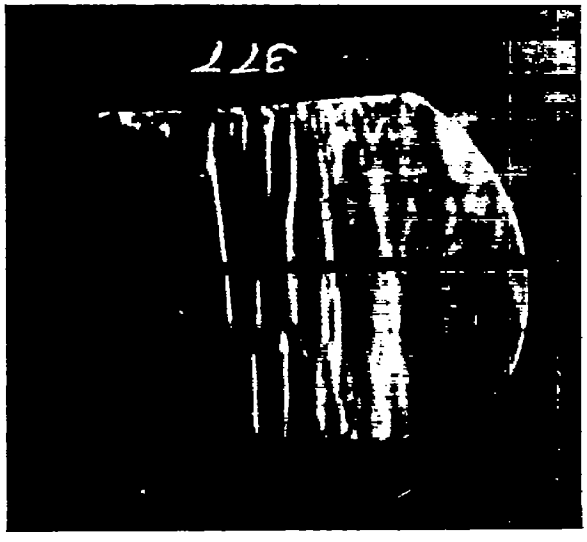

(b) Non-steady shock waves at nozzle throat. Exposure 4 microseconds. Turbulence is probably responsible for this non-steady phenomena.

Figure 17.—Schlieren photographs of air flow through a nozzle.

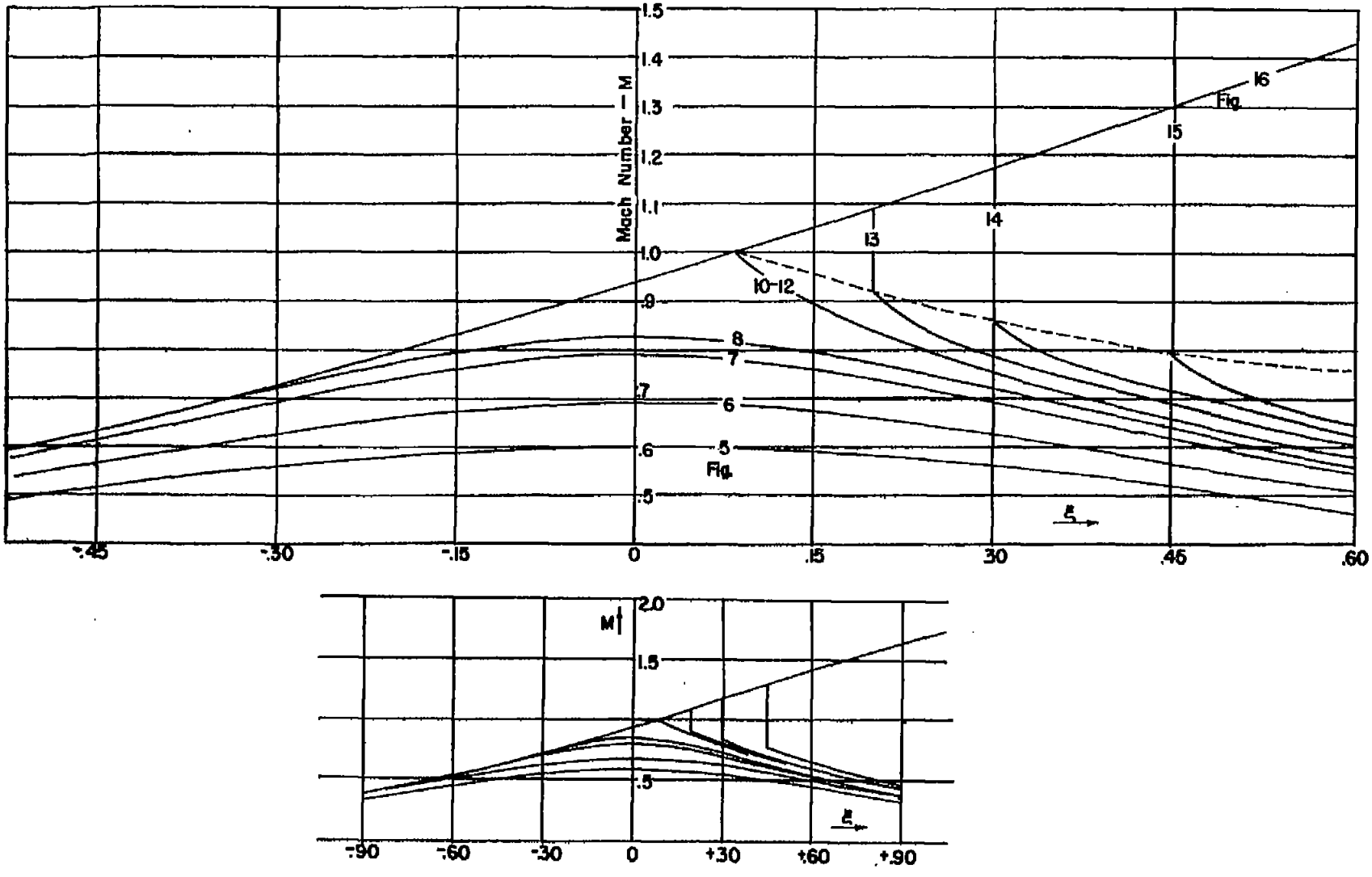

Figure 18.- Mach number along the center line.

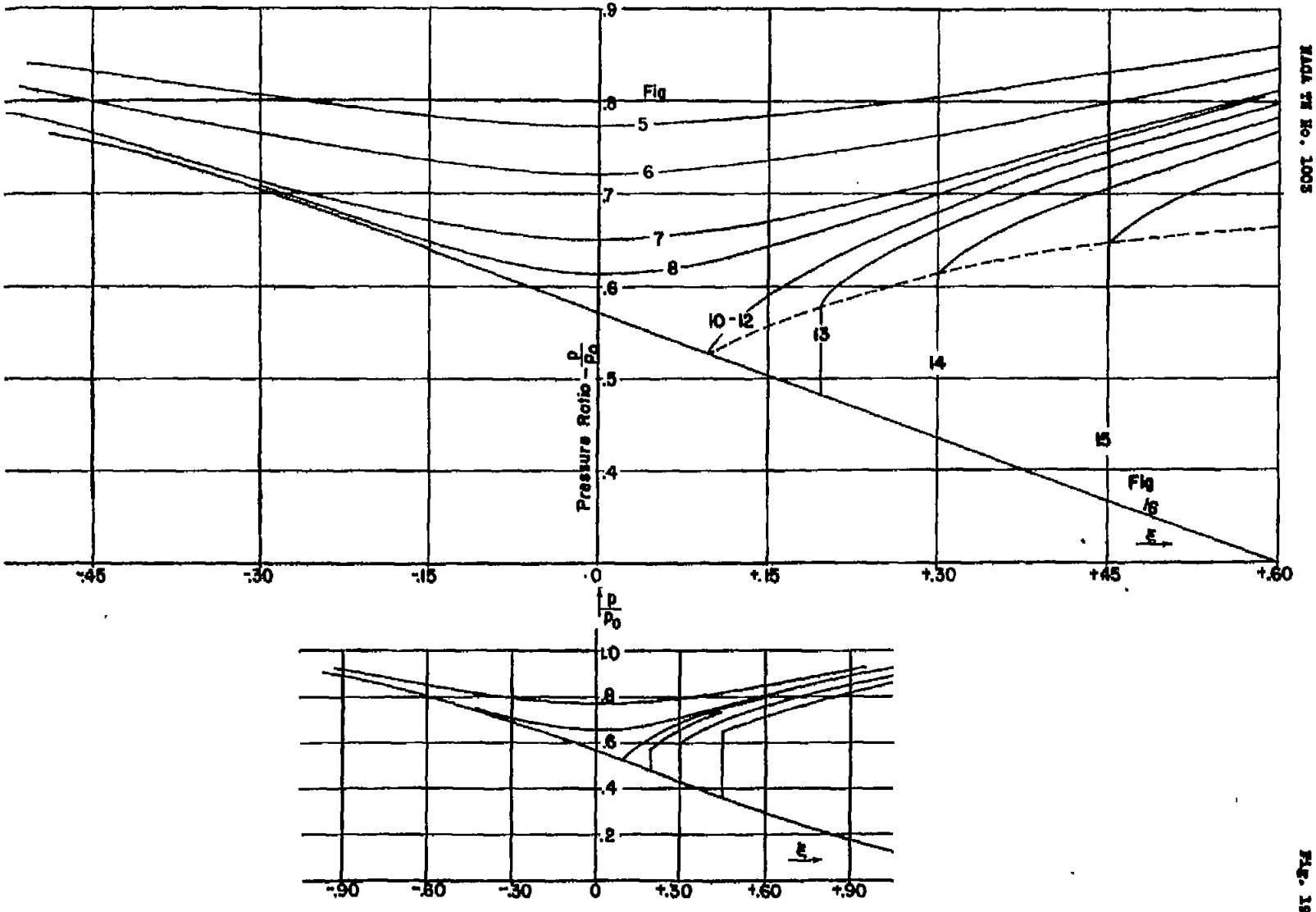

Figure 19.- Pressure ratio along the center line.

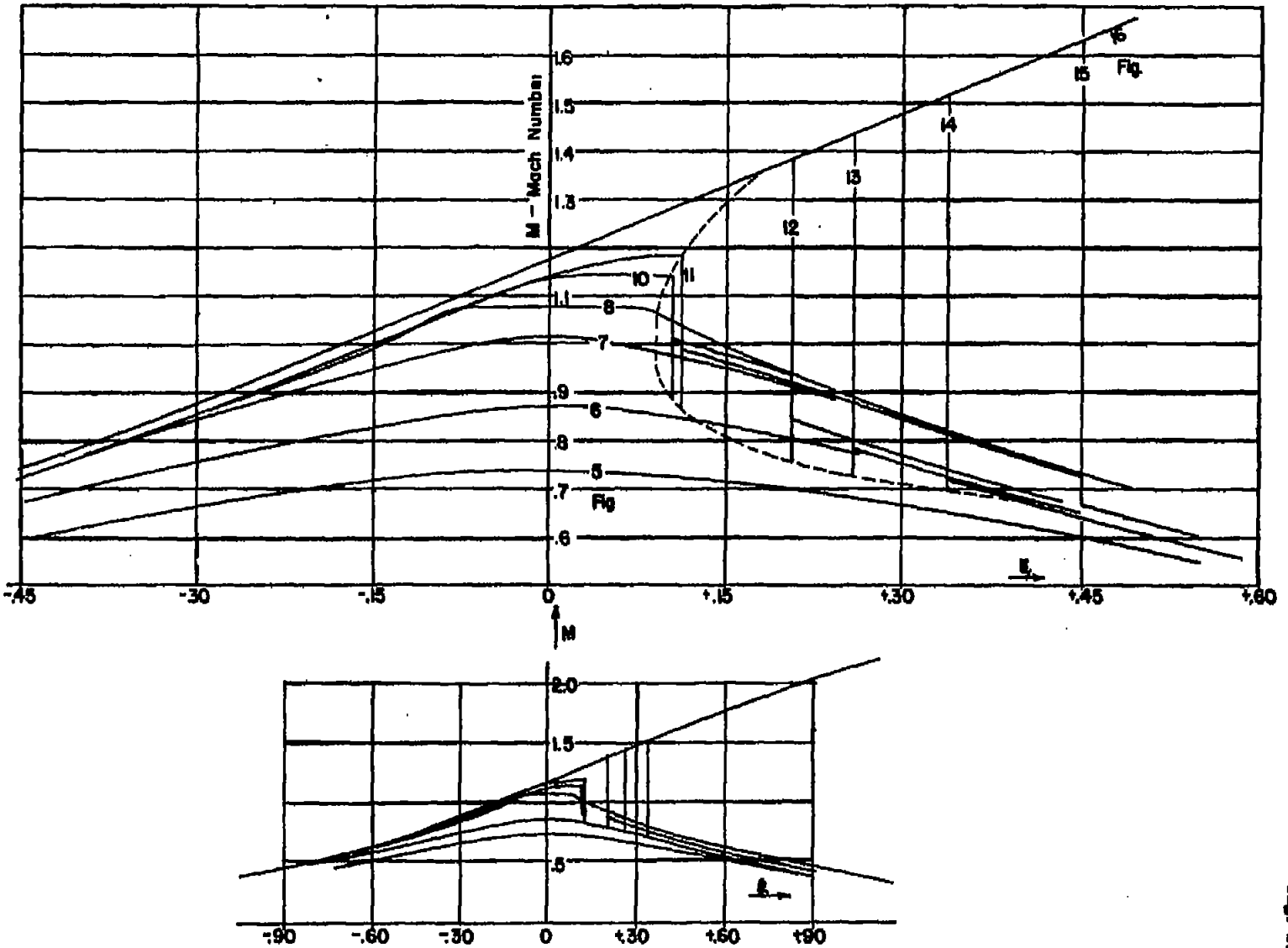

Figure 20.- Mach number along the wall.

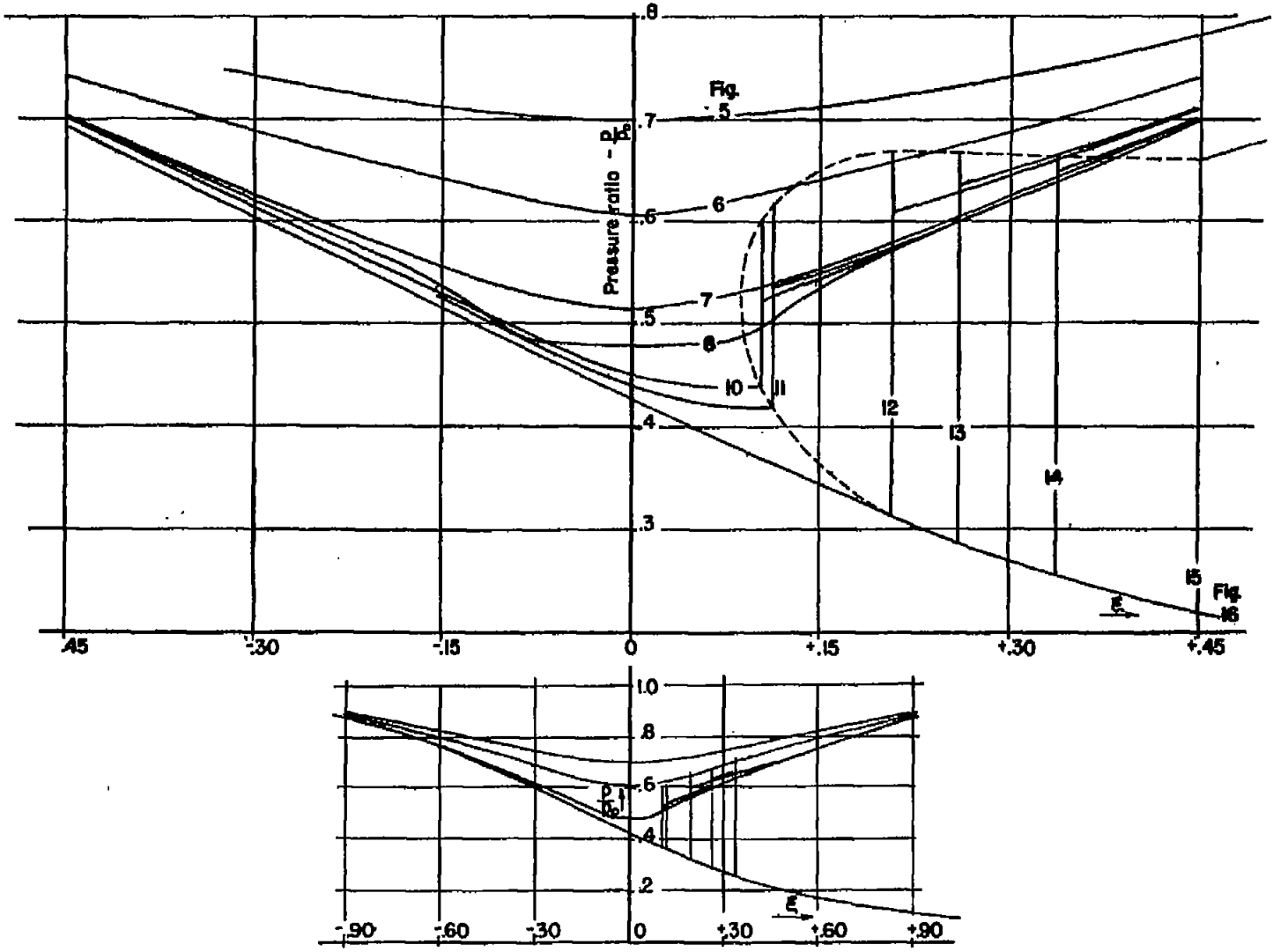

Figure 21.- Pressure ratio along the wall.

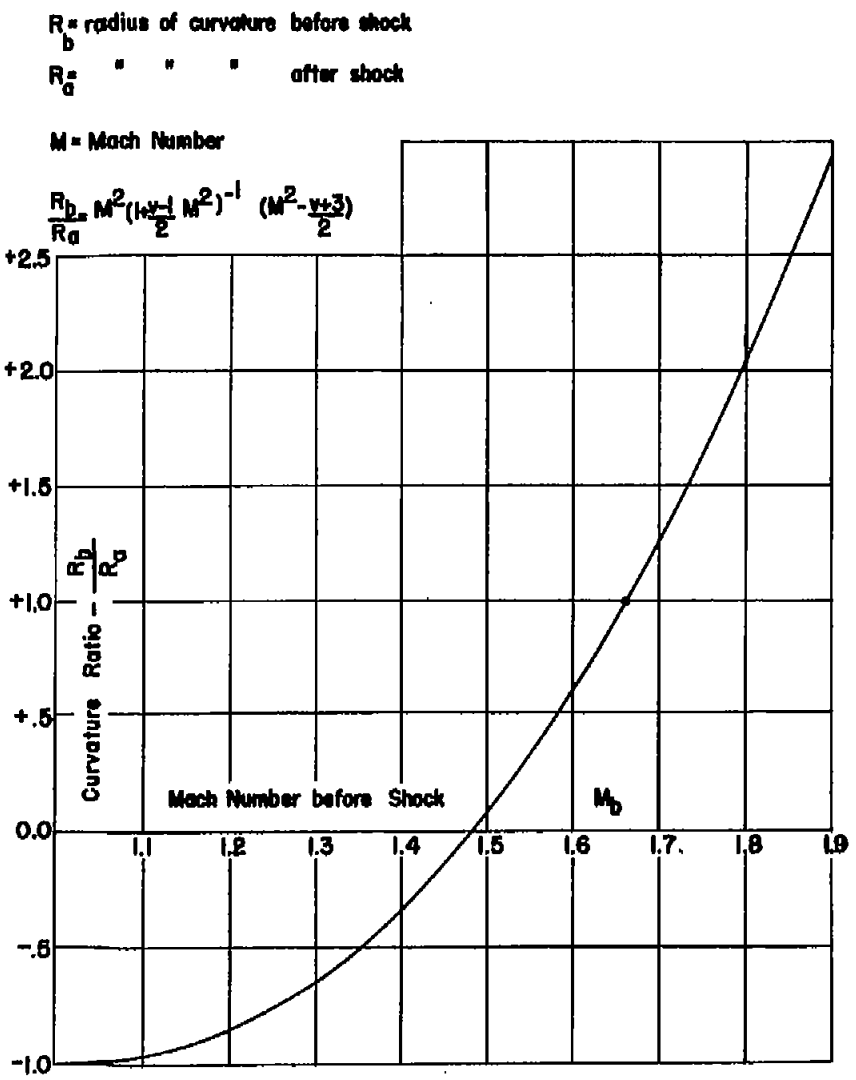

Figure 22.- Change of curvature through a normal shock against Mach number.

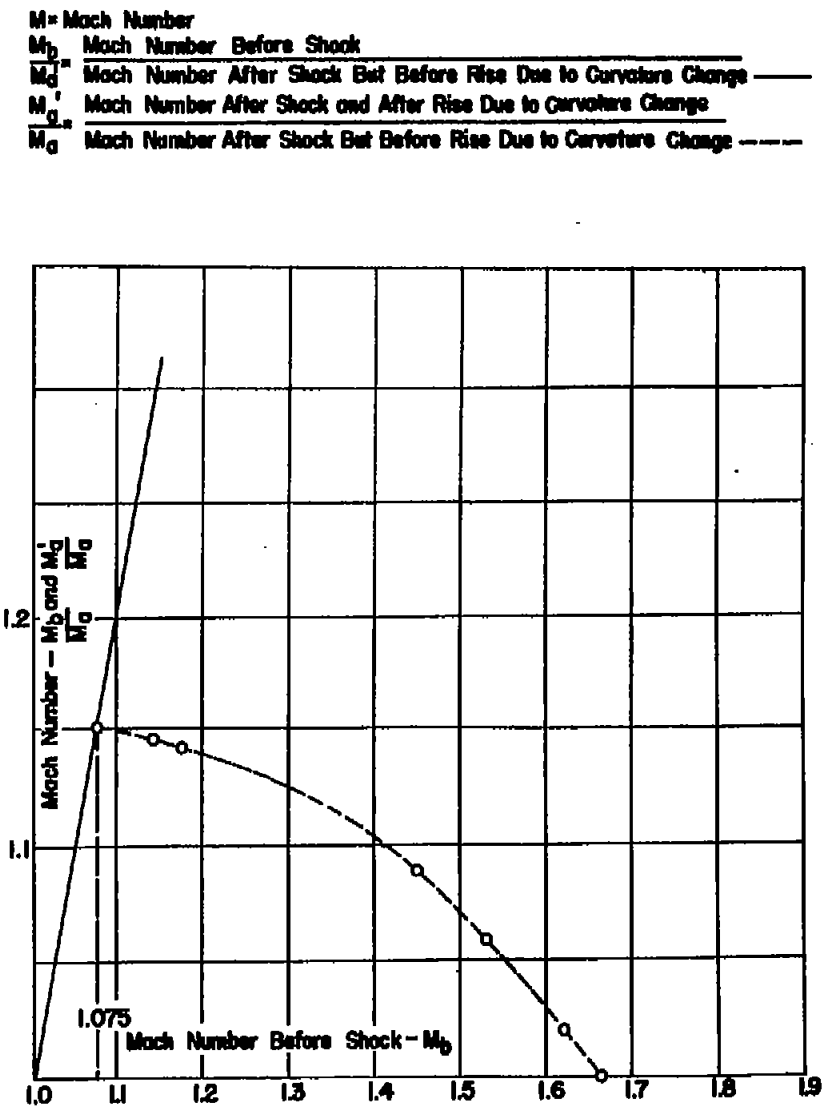

Figure 23.- Mach number ratio through normal shock at the wall of channel.

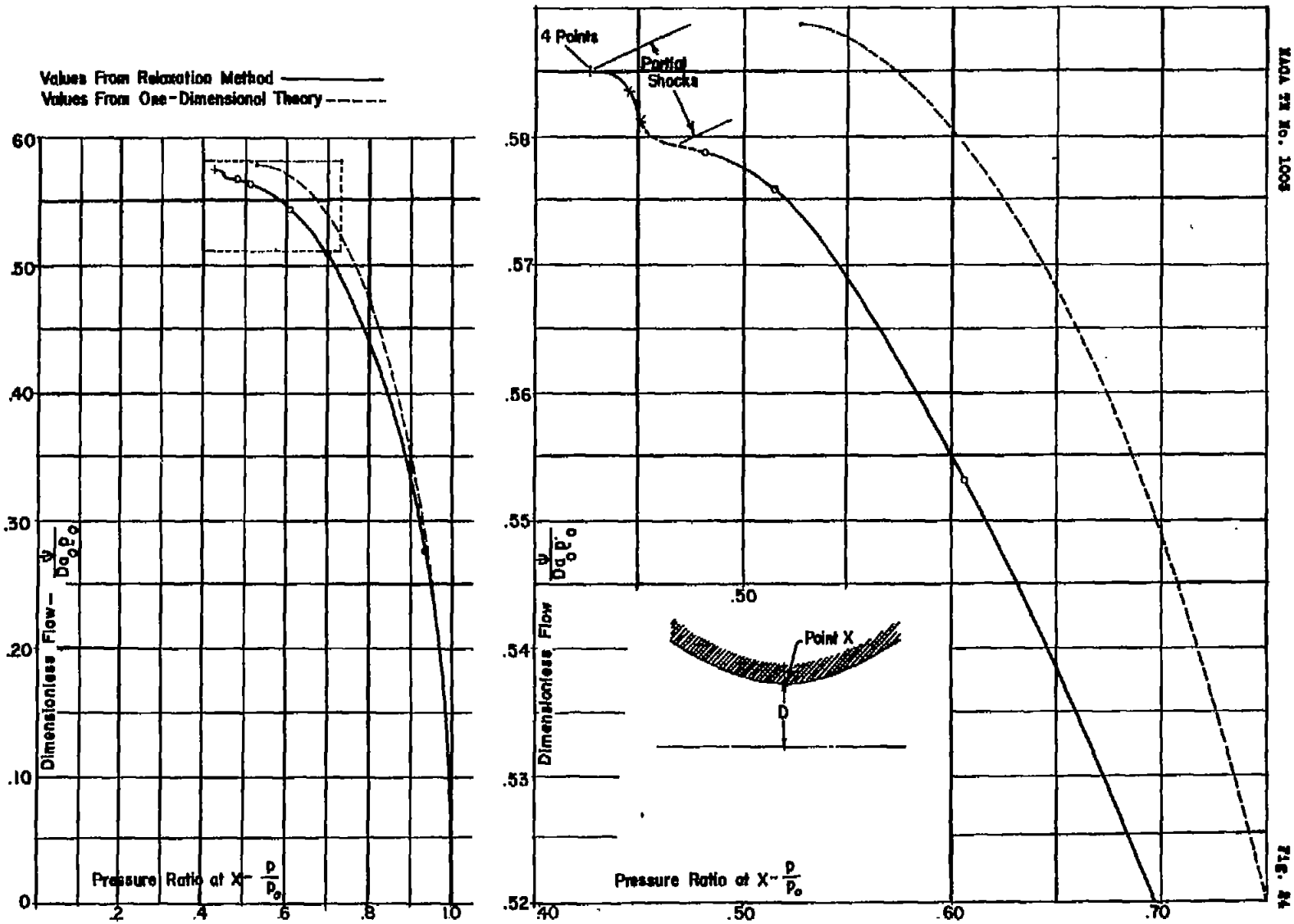

Figure 24.- Dimensionless flow against pressure ratio at point X on the wall. Coordinates of point X: $\xi = 0$; $\eta = 6$.

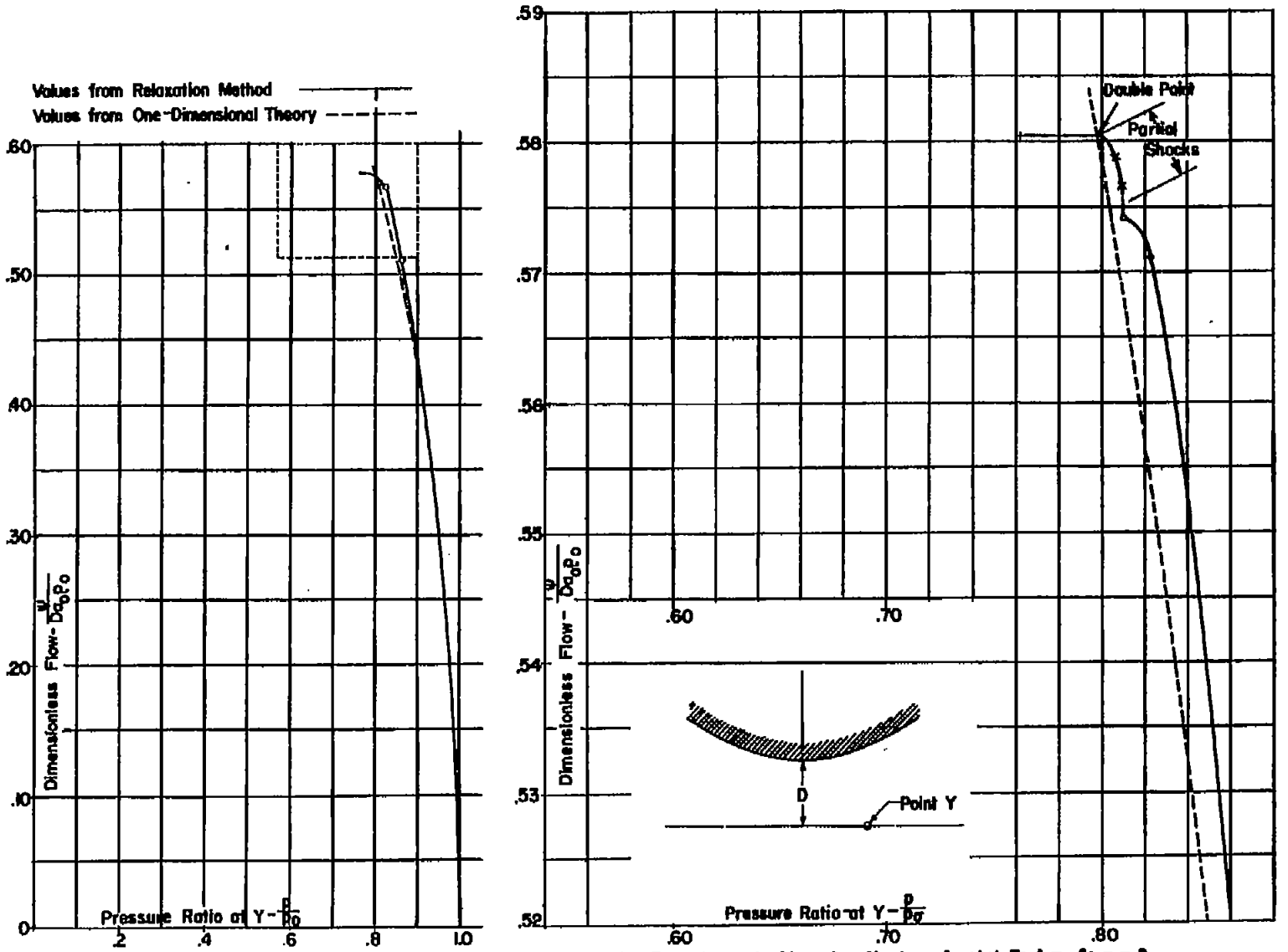

Figure 25.- Dimensionless flow against pressure ratio at point Y on the centerline. Coordinates of point Y: $\xi = .6$; $\eta = 0$.

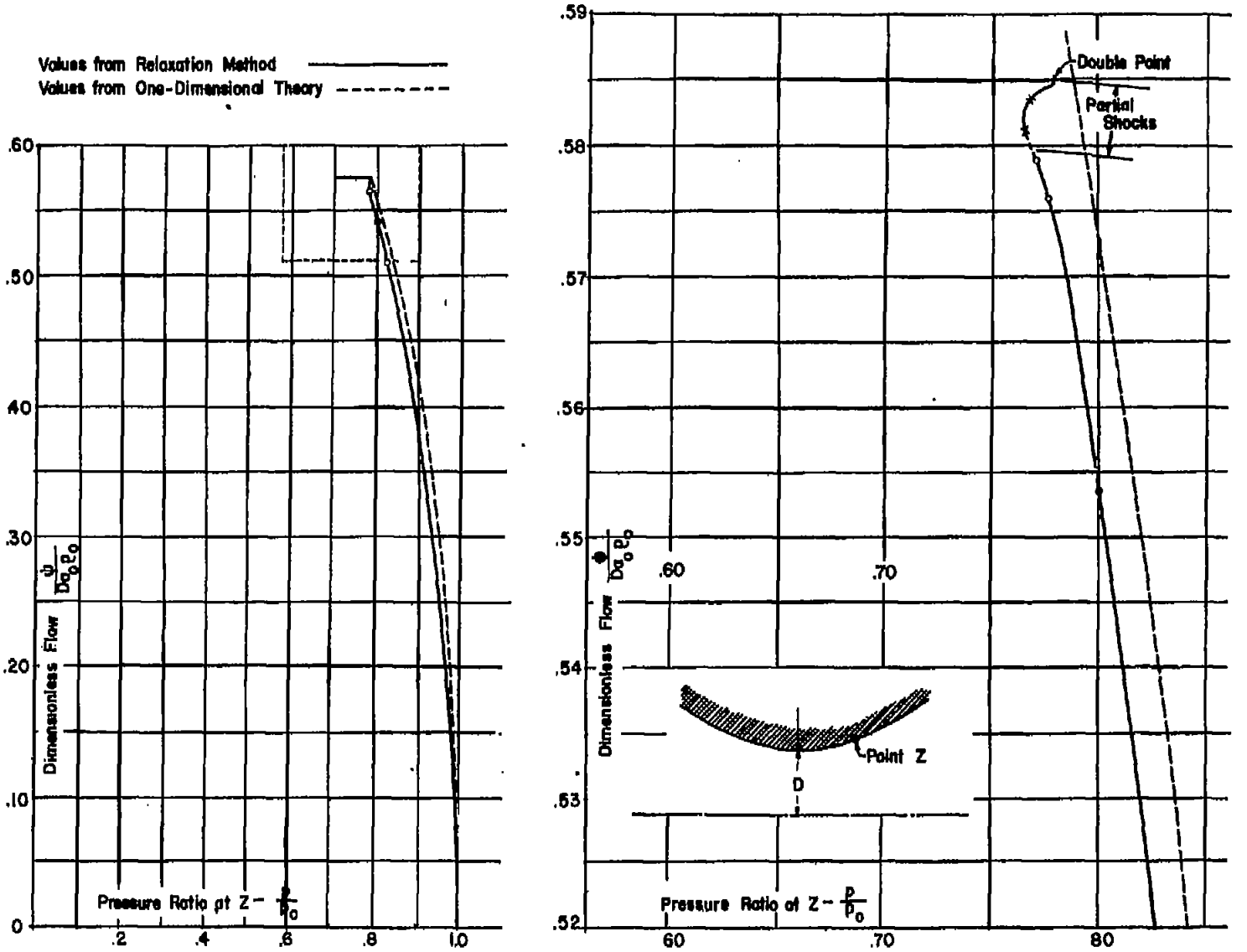

Figure 26.- Dimensionless flow against pressure ratio at point Z on the wall. Coordinates of point Z: ξ = .6; η = .6.

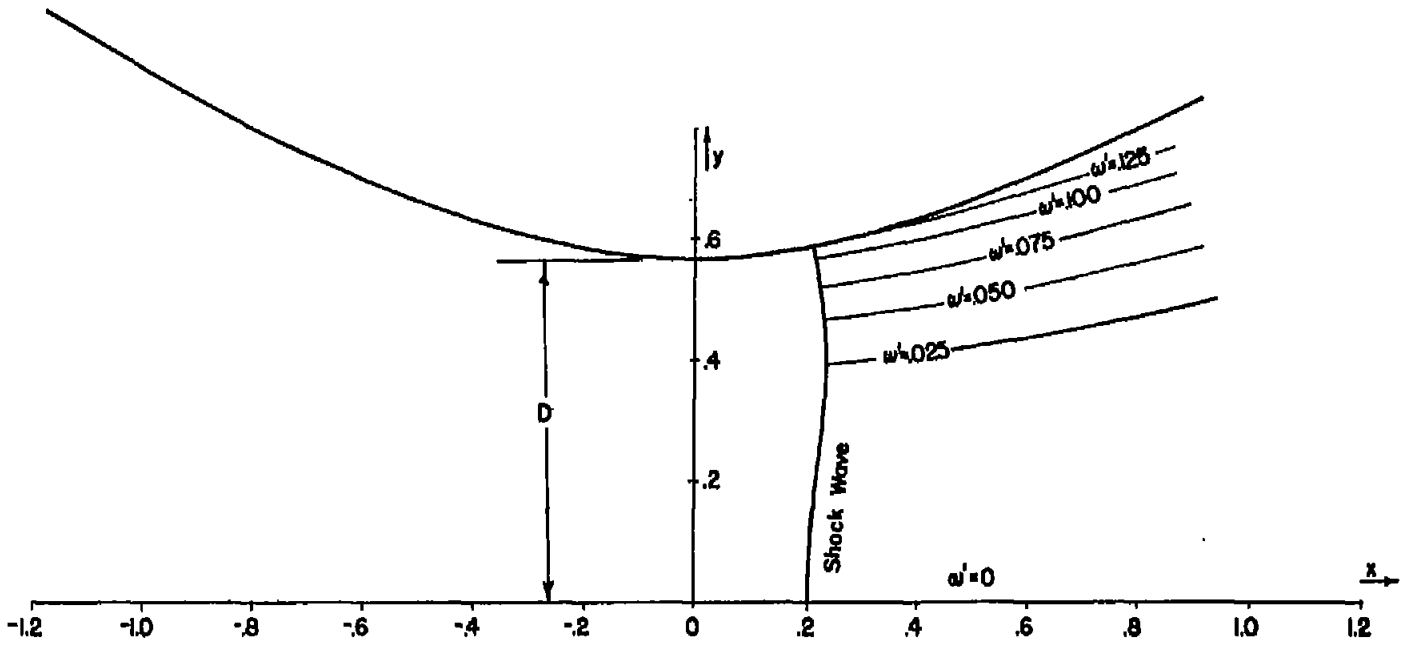

Figure 27.- Flow of compressible fluid in hyperbolic channel; distribution of rotation; constant rotation lines; ω = rotation; $\omega' = \omega D/a_0$, dimensionless rotation; streamlines, constant Mach number lines on figure 13.

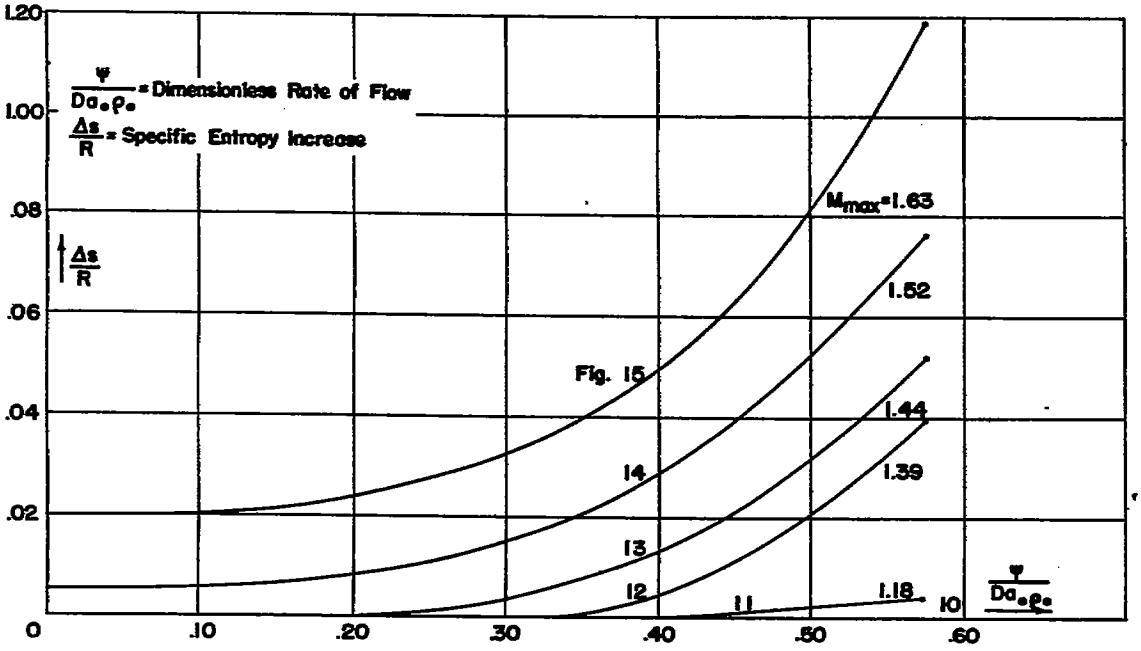

Figure 28.- Specific entropy change against rate of flow. For parameter the maximum Mach number in the channel is used.

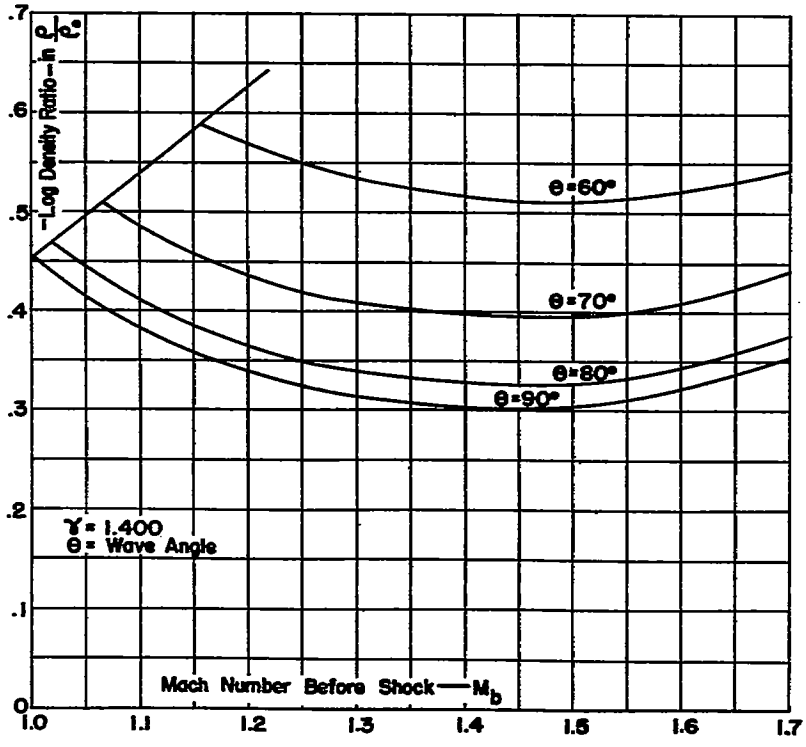

Figure 33.- Computation curve. Log density ratio after shock against Mach number before shock and shock angle.

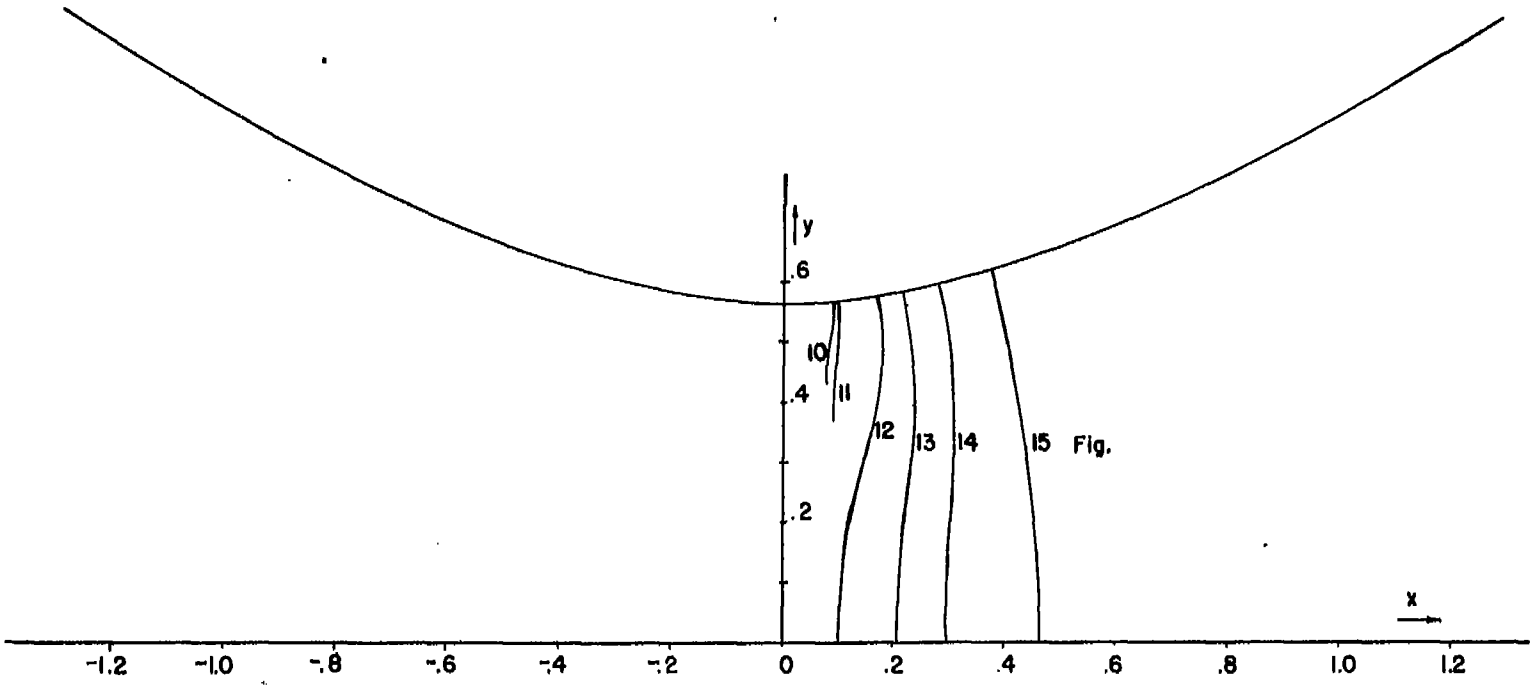

Figure 29.- Flow of compressible fluid in hyperbolic channel and location of different shock waves.

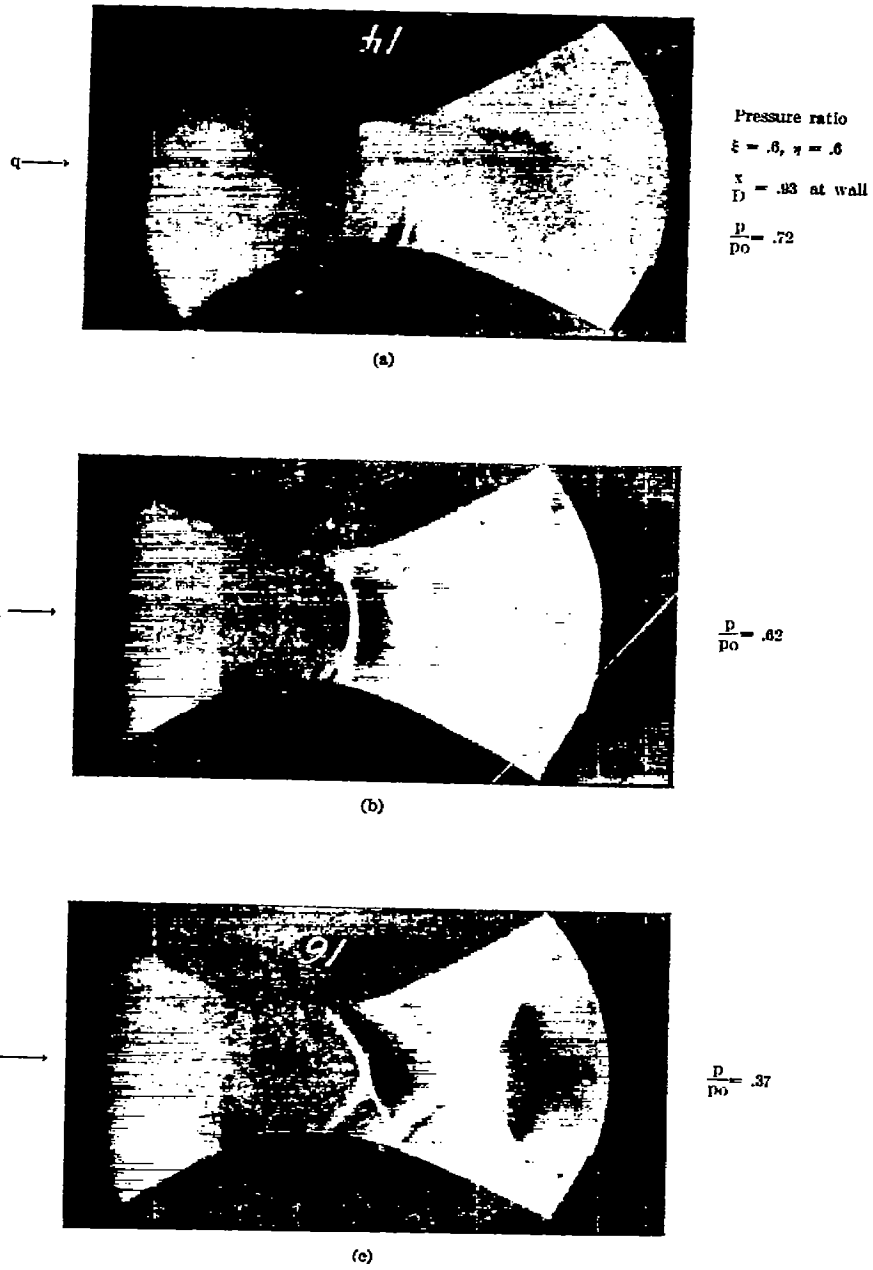

Figure 30.—Schlieren photographs of air flow through hyperbolic channel, flow left to right

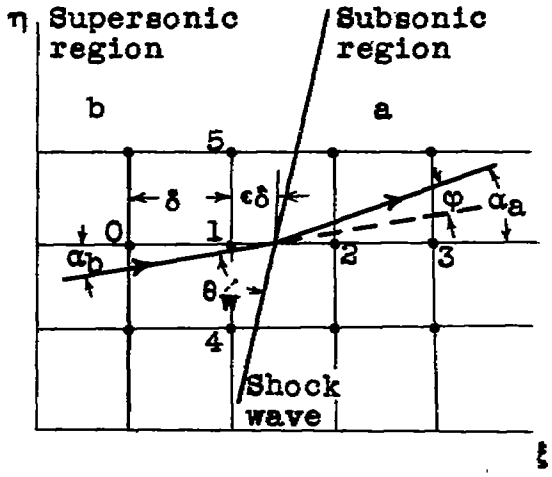

Figure 31.

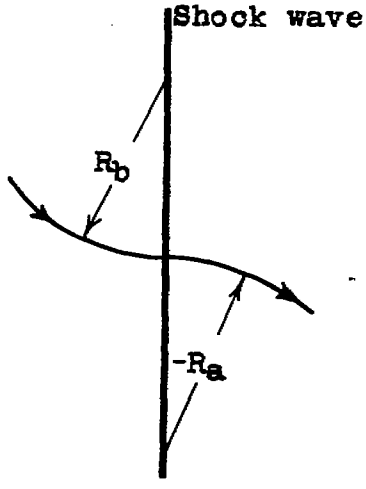

Figure 32.

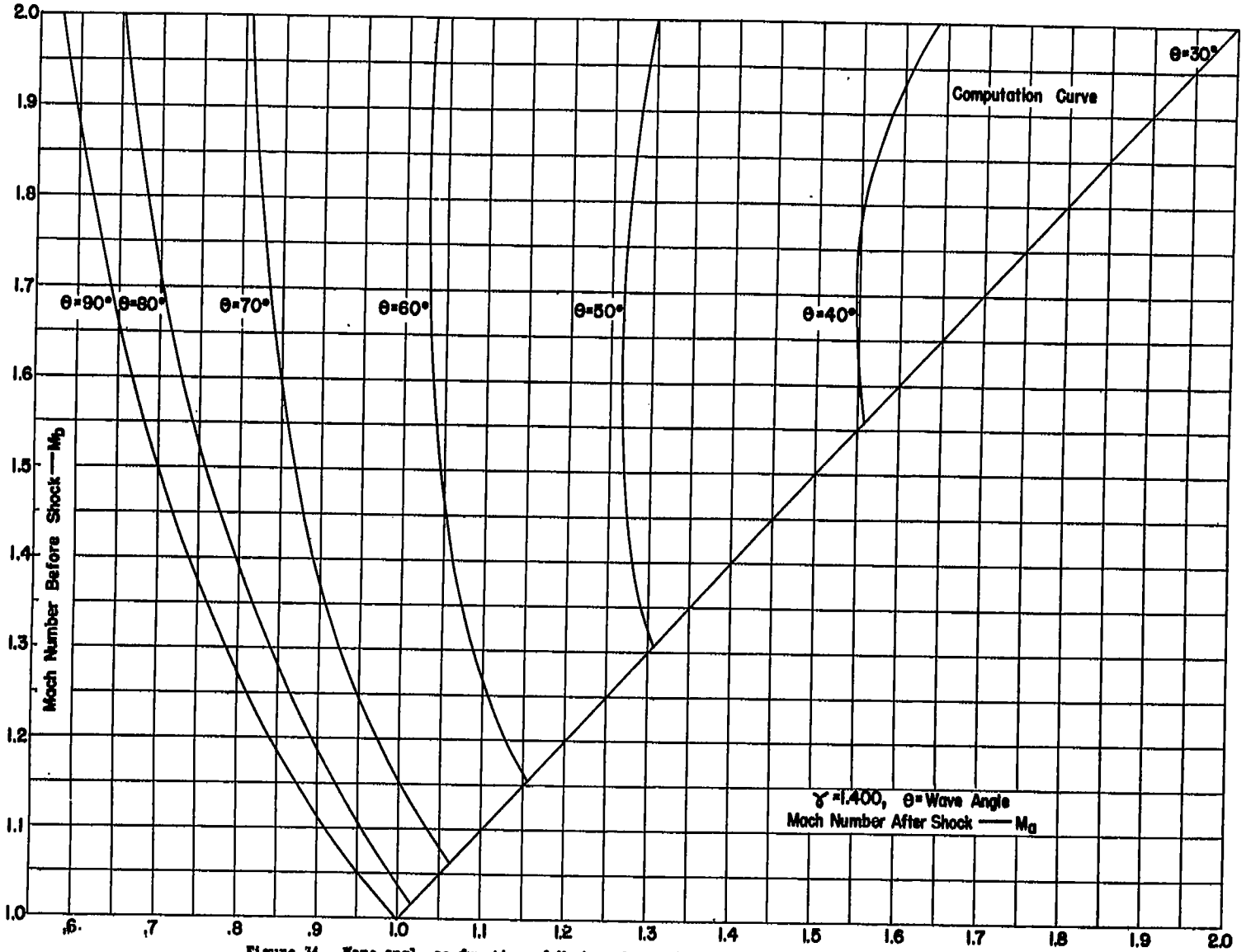

Figure 34.- Wave angle as function of Mach number before shock and Mach number after shock.